Sources of nonlinearities, chatter generation and suppression in metal cutting

Marian Wiercigroch, Erhan Budak

Sources of nonlinearities, chatter generation and suppression in metal cutting

By Marian Wiercigroch[1] and Erhan Budak[2]

[1]*Department of Engineering, King's College,*
University of Aberdeen, Aberdeen AB24 3UE, UK
[2]*Department of Manufacturing Systems Engineering,*
Sabanci University, Istanbul, Turkey

The mechanics of chip formation has been revisited in order to understand functional relationships between the process and the technological parameters. This has led to the necessity of considering the chip-formation process as highly nonlinear, with complex interrelations between its dynamics and thermodynamics. In this paper a critical review of the state of the art of modelling and the experimental investigations is outlined with a view to how the nonlinear dynamics perception can help to capture the major phenomena causing instabilities (chatter) in machining operations. The paper is concluded with a case study, where stability of a milling process is investigated in detail, using an analytical model which results in an explicit relation for the stability limit. The model is very practical for the generation of the stability lobe diagrams, which is time consuming when using numerical methods. The extension of the model to the stability analysis of variable pitch cutting tools is also given. The application and verification of the method are demonstrated by several examples.

Keywords: metal cutting; nonlinear dynamics; chatter; chip formation

1. Introduction—why metal cutting?

Machining (in particular, metal cutting) is still the fundamental manufacturing technique and it is expected to remain so for the next few decades. Moreover, it is predicted that ultra-precision machining will take an even more significant role among other manufacturing techniques. According to the International Institution for Production Research (CIRP), machining accounts for approximately half of all manufacturing techniques, which is a reflection of the achieved accuracy, productivity, reliability and energy consumption of this technique. While considering the automated manufacturing centres, manufacturing flexibility brings an additional important advantage.

However, addressing new challenges, such as environmental issues and cost reduction, while improving quality of final products, drives metal machining research into two directions, namely ultra-precision metal cutting and high-speed metal cutting. The former is strictly related to the current advancement in cutting-tool technology, where, due to the use of diamond tools, their geometries and the material properties, there has been a significant reduction in tool wear and breakage. This has put ultra-precision machining in the dominant position in the finishing technologies market. A similar advantage is offered for high-speed metal cutting, due to low specific cutting
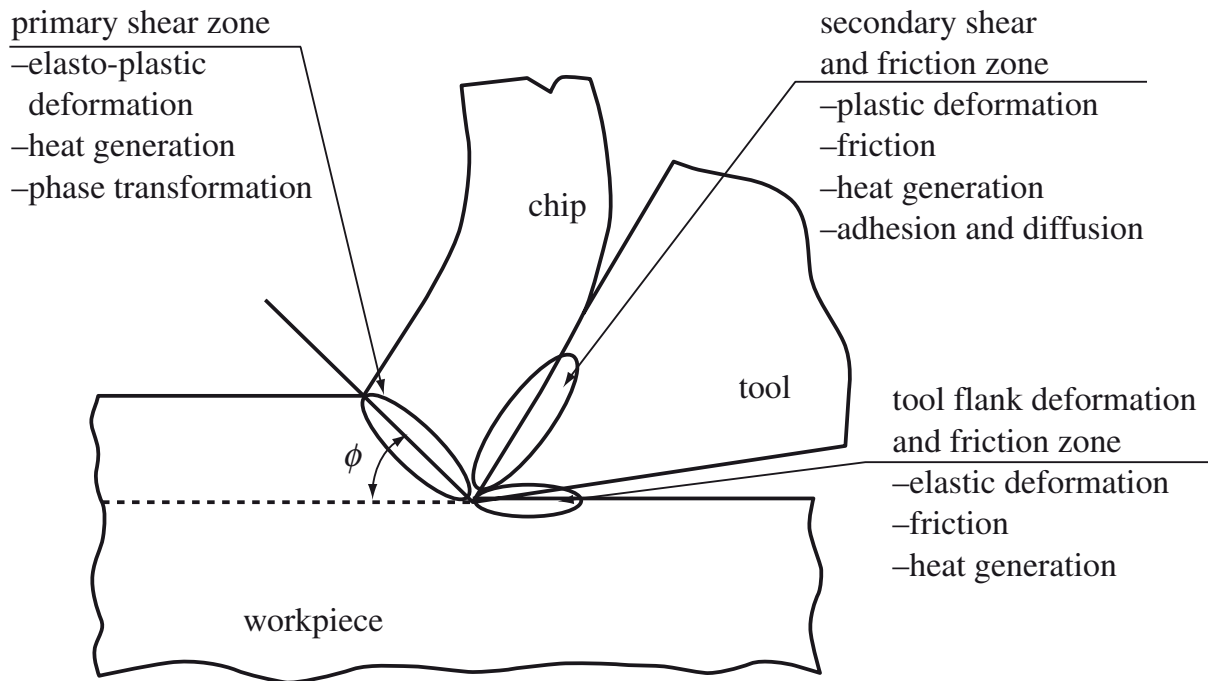
Figure 1. Physical phenomena in the cutting zone.

energy consumption, resulting in smaller cutting forces at high cutting speeds, where the machine tools are pushed to operate at very high RPM, often above the spindle main resonance corresponding to high stability. Since the dynamic stiffness of the machine tool is being explored in such a way, all process and structural nonlinearities having influence on the dynamic stiffness must be appropriately evaluated and included.

In the search for a significant improvement in accuracy and productivity of machining processes, the mechanics of chip formation has been revisited in order to understand functional relationships between the process and the technological parameters. This has led to the necessity of considering the chip-formation process to be highly nonlinear with complex interrelations between its dynamics and thermodynamics. The understanding of these relations will be reflected in the design of new machine tools, not necessarily heavier and stiffer, accommodating the needs of the current competition race for more accurate, productive and cheaper technologies. However, the major requirement is to perform the technological operation under chatter-free conditions, which can guarantee achieving the required geometry and surface finish of the machined parts.

In this paper, a detailed account of the state of the art in modelling and experimental investigations of the cutting-process mechanics and different chatter mechanisms will be provided. To conclude, a practical case study will be given, where the stability of a milling process is investigated using an analytical model.

2. Cutting-process mechanics

(a) Physical phenomena in the cutting zone

In general, the cutting process is a result of the dynamic interactions between the machine tool, the cutting tool and the workpiece. Therefore, its mathematical description should take into account its kinematics, dynamics, geometry of the chip formation and workpiece mechanical and thermodynamical properties. Mechanics of the cutting process and chip formation is recognized even more now than ever before
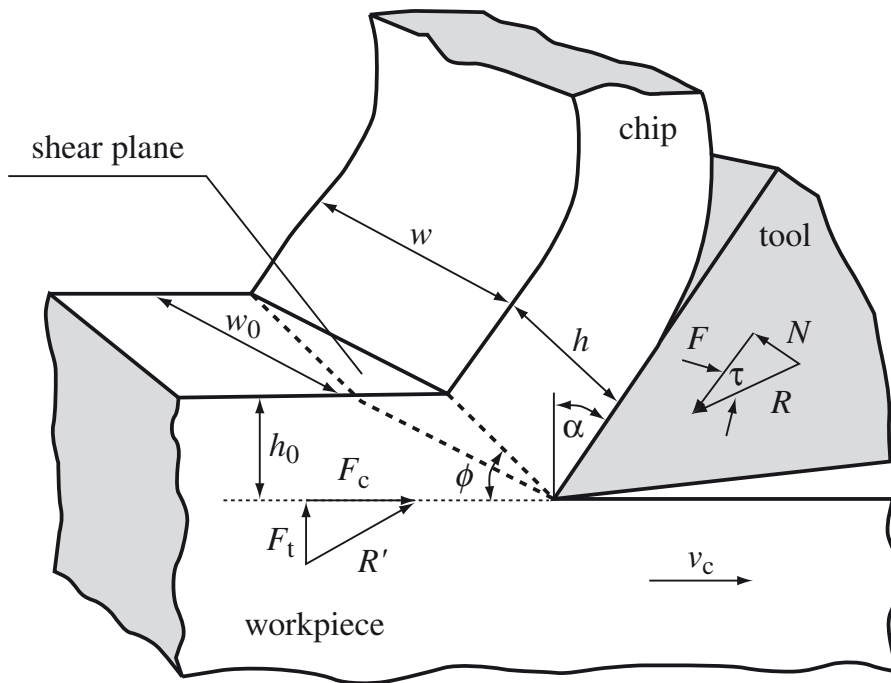
Figure 2. Model of orthogonal metal cutting.

as the key issue in the development of machining technologies. The complexity of the cutting process is due to the interwoven physical phenomena such as elasto-plastic deformations in the cutting zones, variable friction between the tool and the chip and the workpiece, heat generation and transfer, adhesion and diffusion, and material structural and phase transformations, to name but a few. A simplified schematic locating all important phenomena in the cutting zone is shown in figure 1. Understanding the relationships between these phenomena is the most important issue in the modelling of the cutting processes. It is worth pointing out here that most of the phenomena listed are strongly nonlinear and interdependent. For example, the friction between the chip and the tool and between the tool and the workpiece is a nonlinear function of the relative velocity. In addition, it generates heat, which, in turn, alters the shear strength and lubrication conditions.

(b) Piispanen's and Merchant's models

Studies on metal-cutting processes were carried out as early as the 1800s. The first significant research work was published by Taylor (1907), and, in the mid-1940s and 1950s, two researches (Piispanen 1937, 1948; Merchant 1944, 1945a,b) described the flow of metal chips. Based on this concept of orthogonal cutting, a continuous chip is formed by a cutting process, which was understood to be confined to a single shear plane extending from the cutting edge to the shear plane. These investigations were restricted to a model of orthogonal or two-dimensional metal cutting, which is shown in figure 2. Here, the uncut layer (initial depth of cut), h_0, of the workpiece in the form of a continuous chip without a built-up edge is seen to be removed along the shear plane. Subsequently, the chip of thickness h flows along the face of the tool, where it encounters friction on the tool–chip interface. The width of the chip remains unchanged, therefore the stress field can be considered in two dimensions. The force system shown is required to plastically deform the uncut layer, h_0, to the final thickness t (Eggleston et al. 1959). The cutting force, F_c and the thrust force, F_t, determine the vector R, which represents the resistance of the material being cut acting on the cutting tool. In stationary cutting conditions, this force is compensated
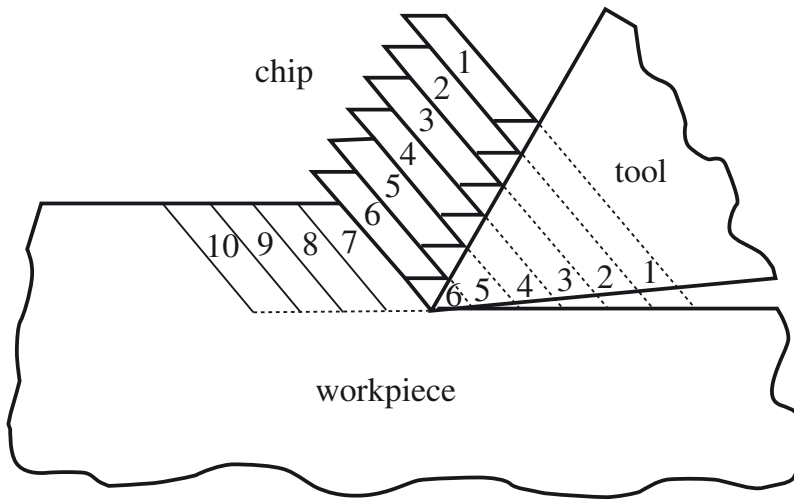
Figure 3. Piispanen's model of chip formation.
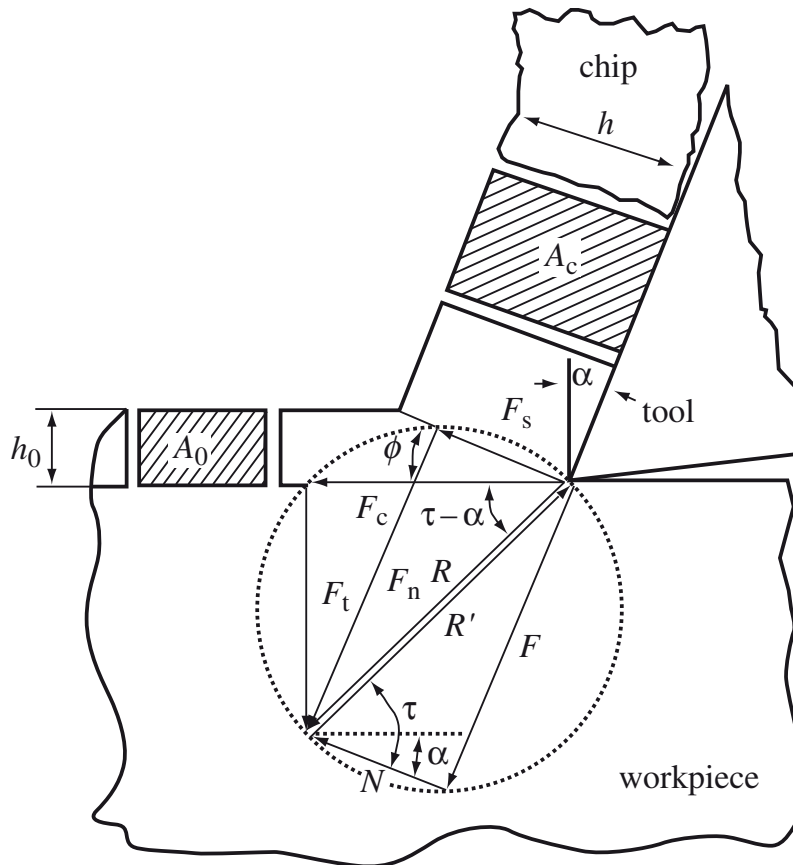
Figure 4. Merchant's force diagram.

by the resultant force generated from the shear stress field, and the friction on the rake surface; the position is determined by the rake angle, α.

The chip-formation mechanism is controlled by instant cutting parameters such as feed, velocity and depth of cut. Any change in these parameters during cutting instantaneously changes the value of the normal force, N, the friction force, F, and the relative velocity between the chip and the workpiece, v_c, thus effecting the dynamics of the system (Wu & Liu 1985a, b).

The process of shear deformation can be illustrated by the successive displacement of cards in a stack, as shown in figure 3. Each card is displaced forward by a small distance with respect to its neighbours as the cutting tool progresses. Establishing a relationship between the card thickness and the relative displacement between the neighbouring cards leads to the shearing strain; the so-called *natural strain* (Merchant 1945a). The product of the natural strain with the mean shear strength of the

4

workpiece gives the work done per volume of metal removed. This concept, which was originally put forward by Piispanen (1937), was later analytically and experimentally investigated by Merchant (1944, 1945a, b). The force diagram developed by Merchant (1944) has been used extensively. The basic idea behind this elegant approach is that the force R coming from the workpiece and acting on the chip is compensated by the force R' coming from the cutting tool. The force vector R' is composed of two components: the cutting force, F_c, and the thrust force, F_t. The material resistance force also has two components: the shearing force, F_s, and the friction force, F_τ, as depicted in figure 4.

The key variable in Merchant's approach (Merchant 1944) is the shear angle, ϕ. By knowing this angle and a few constant process parameters, the force R can be calculated from

$$R = \frac{F_s}{\cos(\tau - \alpha + \phi)}, \tag{2.1}$$

where $F_s = \sigma_s A_s$, A_s is the cross-section of the shear plane, σ_s is the shear flow stress, and α and τ are the rake and friction angles, respectively. The cross-section A_s can be also expressed in terms of the shear angle as $A_s = wh/\sin\phi$, which leads to the formula

$$R = \frac{\sigma_s w h_0}{\cos(\tau - \alpha + \phi)\sin\phi}. \tag{2.2}$$

Having established (2.2), the cutting and thrust forces can be evaluated from the following equations:

$$F_c = R\cos(\tau - \alpha) = \sigma_s w h_0 \frac{\cos(\tau - \alpha)}{\cos(\tau - \alpha + \phi)\sin\phi}, \tag{2.3}$$

$$F_t = R\sin(\tau - \alpha) = \sigma_s w h_0 \frac{\sin(\tau - \alpha)}{\cos(\tau - \alpha + \phi)\sin\phi}. \tag{2.4}$$

In the Merchant's approach, it was assumed that the cutting-process mechanics could be entirely explained by the angle ϕ. This has led to the determination of the optimum shear angle, which is based on the minimum-energy principle (Merchant 1945a), as

$$\phi = \tfrac{1}{4}\pi - \tau + \alpha. \tag{2.5}$$

This simple formula allows us to determine the friction angle τ by a direct measurement of the shear angle ϕ. By substituting the above equation (2.5) in the formulae for the cutting and the thrust forces, equations (2.3) and (2.4) lead to

$$F_c = \sigma_s w h_0 \frac{\cos(\tau - \alpha)}{\sin^2\phi}, \tag{2.6}$$

$$F_t = \sigma_s w h_0 \frac{\sin(\tau - \alpha)}{\sin^2\phi}. \tag{2.7}$$

As has been demonstrated, Merchant developed an elegant model based on the shear angle, and despite of the fact that this approach has not correlated too well with the experimental results, this research left a significant impact in the field.
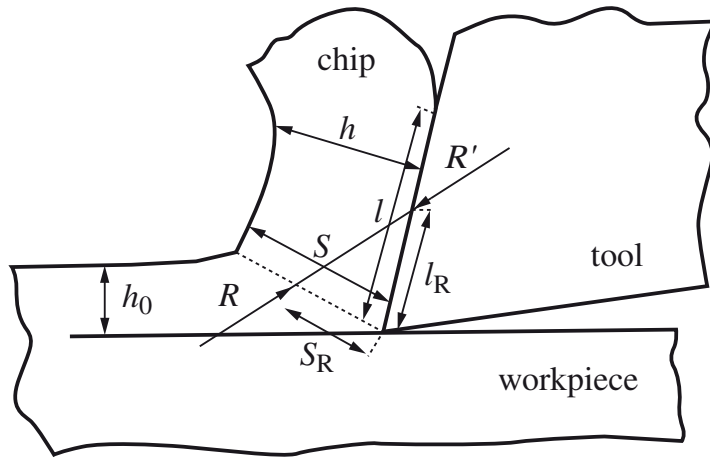
Figure 5. Schematic for calculation of the shear angle, ϕ.

(c) Kudinov's model

The model of *dynamic cutting characteristics* developed by Kudinov (1955, 1963, 1967) has been widely used in the former Soviet Union and Eastern Europe. It assumes that chatter and variation of the cutting and thrust forces are due to the dynamic changes of chip thickness and relative kinematics between the tool and workpiece. The starting point of his scheme is the cutting force, F_c, which is evaluated for steady-state conditions from the following semi-empirical formula given by Loladze (1952),

$$F_c = C_c \sigma w \xi h_0, \tag{2.8}$$

where C_c and $\xi = h/h_0$ are the material constant and the chip-thickness ratio, respectively. Assuming an arbitrary depth of cut, h, the above equation takes the form

$$F_c = C_c \sigma w h. \tag{2.9}$$

If the material properties remain unchanged, a dynamic component of the cutting force can be calculated by differentiating the steady-state force, with h and ξ as independent variables,

$$dF_c = C_c \sigma w(\xi_0 \, dh + h_0 \, d\xi), \tag{2.10}$$

where h_0 and ξ_0 are nominal values of the depth of cut and chip-thickness ratio. The chip-thickness ratio can be calculated from the chip geometry (see figure 5a) as

$$\xi = \cot\phi \cos\alpha + \sin\alpha. \tag{2.11}$$

To evaluate the shear angle, ϕ, a formula developed by Zorev (1956) based on the force equilibrium on the shear plane and rake surface was used,

$$l = \frac{m}{n}[\tan\tau + \tan(\phi - \alpha)]h, \tag{2.12}$$

where $m = s_R/s$, $n = l_R/l$, and the distances l, l_R, s and s_R are shown in figure 5.

It was experimentally observed (Kudinov 1963, 1967) that the ratio m/n is kept constant in a wide range of the contact length variation. Also, it was assumed that $\tan\tau + \tan(\phi - \alpha) \approx \tan\phi$, which, in the authors' view, has neither strong physical nor mathematical justification. This has led to an approximate relationship between the shear angle, and the chip thickness and contact length,

$$\cot\phi = \frac{m}{n}\frac{h}{l}. \tag{2.13}$$

6

Equations (2.12) and (2.13) have been obtained for a steady-state cutting process. If the process is unsteady, i.e. the depth of cut and chip contact length vary, the following formula was proposed by Kudinov (1967),

$$\mathrm{d}l = \frac{m}{n}[\tan\tau + \tan(\phi - \alpha)]\,\mathrm{d}h, \tag{2.14}$$

which, in fact, is a total differential of equation (2.12). Assuming, as previously, that $\tan\tau + \tan(\phi - \alpha) \approx \tan\phi$ leads to

$$\cot\phi = \frac{m}{n}\frac{\mathrm{d}h}{\mathrm{d}l}. \tag{2.15}$$

For the general case, the following approximate formula was proposed to describe the relationship between the shear angle, ϕ, and two independent variables such as $\mathrm{d}h/\mathrm{d}l$ and α:

$$\cot\phi \approx \frac{m}{n}\frac{1}{1 + (m/n)(\mathrm{d}h/\mathrm{d}l)(\alpha - \tau)}. \tag{2.16}$$

Taking a total differential of the above equation and assuming that the chip velocity is almost constant for small chip-thickness variations, i.e.

$$\mathrm{d}l = \frac{v_c}{\xi_0}\,\mathrm{d}t, \tag{2.17}$$

leads to a relationship for $\mathrm{d}\xi$, which, in turn, is substituted into (2.10). This finally allows us to obtain the expression for the cutting force, F_c. As the last part of the original derivation is not rigorous (and even confusing), the authors have taken the liberty of sketching a simple substitute. Thus one can compute a total differential of (2.15) as

$$\mathrm{d}\cot\phi = \frac{m}{n}\mathrm{d}\left(\frac{\mathrm{d}h}{\mathrm{d}l}\right). \tag{2.18}$$

Assuming a small angle α and calculating a total differential of (2.11) leads to

$$\mathrm{d}\xi = \mathrm{d}\cot\phi. \tag{2.19}$$

This, together with (2.17), is substituted first into (2.18) and then into (2.10) to obtain the formula for a dynamic change of the cutting force,

$$\mathrm{d}F_c = C_c\sigma w\left(\xi_0\,\mathrm{d}h + h_0\frac{m}{n}\frac{\xi_0}{v_c}\,\mathrm{d}^2h\right). \tag{2.20}$$

Similarly, an expression for a dynamic thrust force can be developed as

$$\mathrm{d}F_t = C_t\sigma w\left(\xi_0\,\mathrm{d}h + h_0\frac{m}{n}\frac{\xi_0}{v_c}\,\mathrm{d}^2h\right), \tag{2.21}$$

where C_t is the thrust force constant.
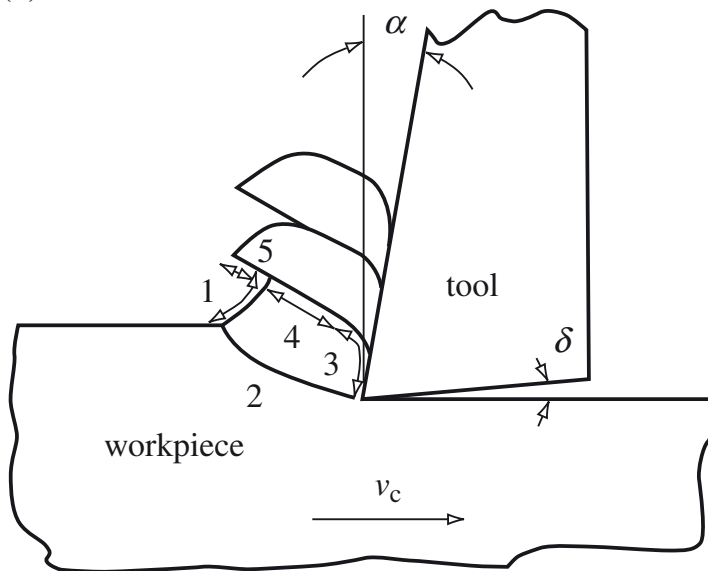
In the original work by Kudinov (1963), equations (2.20) and (2.21) are transformed to the Laplace space

$$F_c = K_F h\frac{1}{1 + T_c p}, \tag{2.22}$$

$$F_t = K_F h\frac{1}{1 + T_t p}, \tag{2.23}$$

where K_F is the cutting coefficient (Kudinov 1955), p is Laplace operator and T_c and T_t are chip-formation time constants for the cutting and thrust forces, respectively.
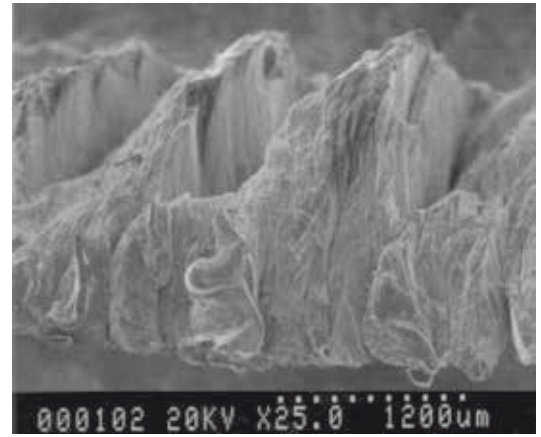
Figure 6. (*a*) Schematic of the segmented chip formation.
(*b*) SEM image of the segmented chip.

(*d*) *Hastings' and Oxley's models*

The main deficiency of the models by Merchant and his earlier followers (e.g. Lee & Shaeffer 1951; Creveling *et al.* 1957; Eggleston *et al.* 1959), and by Kudinov (1963) was a difficulty to verify the theoretical predictions with the experiments. This was mainly due to the fact that the chip-formation process was represented by a single velocity discontinuity, as has been rightly pointed out in a paper by Hastings *et al.* (1980).

The later work by Thomsen's group (e.g. Cumming *et al.* 1965), where a plastic deformation zone and nonlinear models were introduced, tried to resolve this problem. However, without a proper account for the temperature- and strain-rate-dependent properties of the workpiece, the explanation of the complicated phenomena is hardly possible. To illustrate the complexity of this problem, a brief description of the chip-fragmentation hypothesis (Recht 1985) is given below.

For certain temperatures and workpiece materials, mechanical properties are not capable of sustaining a steady-stress field and chip segmentation, and the resulting fluctuating stress and temperature fields occur. Referring to figure 6*a*, as the workpiece is approached by the tool, it experiences a stress field, which changes with time. The chip segment enclosed within lines 1, 3, 4 and 5 is being plastically deformed by the tool, and stress, strain and temperature fields are building up in the workpiece. As the material begins to shear along line 5, these fields develop conditions leading to thermoplastic instability, and a very thin shear-localized band absorbs the bulk of further strain. Then the chip segment moves up the ramp formed by the workpiece material on the workpiece side of line 5. As the tool moves into the ramp, a new segment begins to form. Its upper surface, represented by line 5, becomes the surface through which the tool upsets the material. As upsetting progresses, this surface becomes that identified by lines 3 and 4, the latter of which is being pressed against the tool face. Until a new localized shear zone forms due to thermostatic instability, the increasing portion of line 4 (a hot sheared surface) that lies on the rake face remains at rest. Shearing between segments along line 3 ceases when the next localized shear zone forms along line 5, due to the build-up of the stress, strain

and temperature fields. Once deformation and shearing have ceased, the chip segments pass up the rake face. Chip-sliding behaviour on the rake face is therefore characterized by a start–stop motion. Considering the pressures, temperatures and heat transfer conditions at the cutting-tool–chip interface, sliding resistance would be expected to be much greater for the segmented chips than for continuous chips. When frictional forces and speed are sufficient to produce localized melting temperatures at asperities within the cutting-tool–chip interface, segmented chips produce much higher friction coefficients, interface temperature and tool wear rates than the continuous chips do. As described above, segmented chips experience stick–slip motion. Under very high compression, molten regions in the interface may quench and freeze. Weld bonds in the interface must be sheared, producing high friction forces. This was confirmed by using scanning electron microscopy to determine a chip-segment surface (figure 6b).

An interesting approach explaining the influence of the temperature- and the strain-rate-dependent properties of the workpiece has been given in the paper by Hastings *et al.* (1980), where plane strain and steady-state conditions as in Merchant's model are considered. For the convenience of further analysis, let us assume an auxiliary angle, $\kappa = \phi + \tau - \alpha$, which, in fact, is the angle between the shear force F_s and the resultant force R. By applying the appropriate stress equilibrium equation along the shear plane, it can be shown that, for $0 < \phi \leqslant \frac{1}{4}\pi$, the angle κ is given by

$$\tan \kappa = 1 + 2(\tfrac{1}{4}\pi - \phi) - Cn, \tag{2.24}$$

in which C is an empirical constant and n is the strain-hardening index calculated from the empirical strain–stress relation

$$\sigma_s = \sigma_1(\theta_{int}, \dot{\gamma}_{int}), \epsilon^n, \tag{2.25}$$

where σ and ϵ are the uniaxial flow stress and strain and σ_1 is a constant defining the stress–strain curve for given values of strain rate, $\dot{\gamma}$, and temperature, θ. The maximum shear strain rate, $\dot{\gamma}_s$, can be calculated from

$$\dot{\gamma}_s = \frac{C v_s}{h_0 \sin \phi}, \tag{2.26}$$

where v_s is the shear velocity. The temperature on the shear plane can be calculated by knowing the initial temperature of the workpiece, θ_w, from the following equation,

$$\theta_s = \theta_w + \eta \frac{1 - \beta(v_c)}{\rho S h_0 w} \frac{F_s \cos \alpha}{\cos(\phi - \alpha)}, \tag{2.27}$$

in which $\eta \in (0, 1)$ is a coefficient accounting for how much of the plastic deformation has occurred on the shear plane, ρ and S are the density and specific capacity of the workpiece, respectively, and $\beta(v_c)$ is the empirical non-dimensional function used to determine a portion of the heat conducted into the workpiece from the shear zone. In a similar manner, the average temperature at the cutting-tool–chip interface, θ_{int}, is calculated

$$\theta_{int} = \theta_w + \frac{1 - \beta(v_c)}{\rho S h_0 w} \frac{F_s \cos \alpha}{\cos(\phi - \alpha)} + \psi \theta_m, \tag{2.28}$$

where θ_m is the maximum temperature rise in the chip and $\psi \in (0, 1)$ is a constant allowing θ_{int} to have an average value. The average temperature rise in the chip, θ_c,
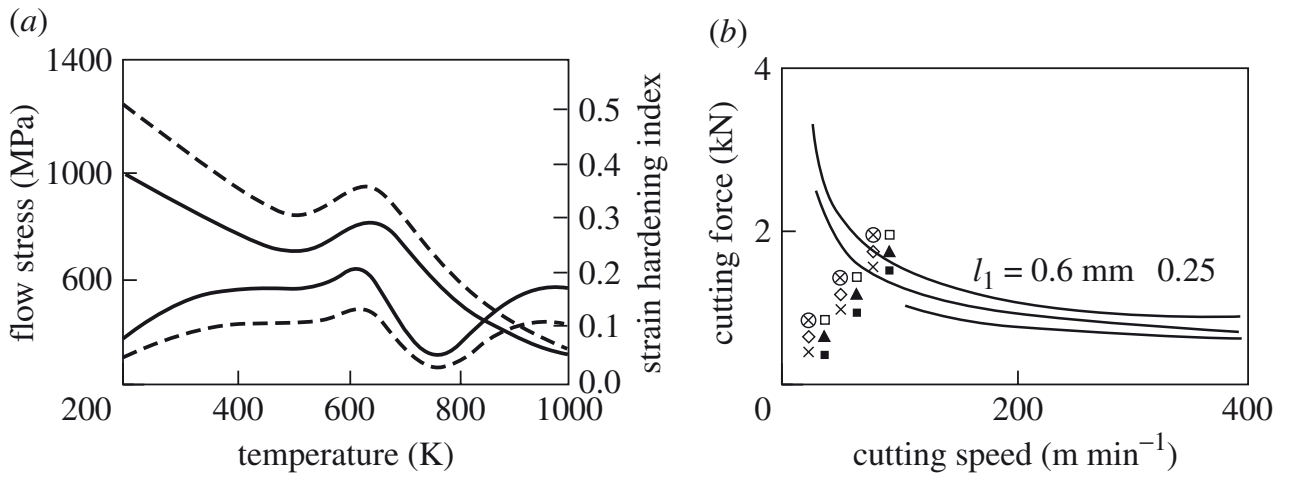
Figure 7. (*a*) Flow stress versus the chip temperature. (*b*) Cutting force against the cutting speed (after Hastings *et al.* 1980).

and the thickness of the plastic zone, δ, can be calculated from a combination of numerical and empirical formulae,

$$\theta_c = \frac{F \sin \phi}{\rho S h w \cos(\phi - \alpha)}, \tag{2.29}$$

$$\log_{10}\left(\frac{\theta_m}{\theta_c}\right) = 0.06 - 0.196\delta\left(\frac{R_\theta h}{l}\right)^{0.5} + 0.5 \log_{10} \frac{R_\theta h}{l}, \tag{2.30}$$

where δ is the ratio between the thickness of the plastic zone in the chip and the chip thickness, R_θ is a non-dimensional thermal coefficient and l is the cutting-tool–chip contact length, which can be calculated from the moment equilibrium on the shear plane,

$$l = \frac{h_0 \sin \kappa}{\cos \lambda \sin \phi}\left(1 + \frac{Cn}{3(1 + 0.5\pi - 2\phi - Cn)}\right). \tag{2.31}$$

To complete this mathematical model, one more equation is required, i.e. a relation for the maximum shear strain rate at the cutting-tool–chip interface

$$\dot{\gamma}_{\text{int}} = \frac{v_c}{\delta h} \frac{\sin \phi}{\cos(\phi - \alpha)}. \tag{2.32}$$

The above set of analytical and empirical expressions allows calculation of the temperature and the strain rate at the cutting-tool–chip interface and the corresponding shear flow stress for the first time. This is then used to determine the cutting and thrust forces from (2.3) and (2.4). The only reservation one should have is the empirical nature of some of the formulae and the fact that the non-monotonic nonlinear relation between the flow stress and the chip temperature (figure 7*a*) is hardly reflected in the cutting/thrust force versus cutting speed characteristics (figure 7*b*).

A similar approach was taken in the paper by Wu (1988), where the mathematical model was constructed perhaps more rigorously. According to the dislocation theory, the shear flow stress is influenced by two effects, namely work-softening and work-hardening (Wright 1982). The work-softening effect is governed by thermal processes mainly dependent on temperature. In turn, the work-hardening mechanism is a function of shear flow strain. A general constitutive law for the shear flow stress is given by the formula

$$\sigma = f(\theta)\gamma^a \dot{\gamma}^b, \tag{2.33}$$

where θ is the temperature, superscripts 'a' and 'b' denote the hardening and shear flow rate exponents, respectively, and $f(\theta)$ is an Arrhenius-type function.

There is a large body of research following these three distinct directions, where additional effects, for example, the waviness of the surface and relative vibration between the tool and the workpiece (e.g. Wu 1986; Lin & Weng 1991), have been introduced. Also, more complex processes, such as oblique cutting or advanced engineering methods (for instance, a finite-element modelling approach by Komvopoulos & Erpenbeck (1991)), have been tried to acquire a deeper insight into the mechanics of the chip formation. It is the authors' view that, despite the significant progress made in perceiving the complex mechanism of the chip formation using linear models, a proper understanding will only be possible when the nonlinear nature of the chip-formation phenomena is unveiled and appropriately modelled.

3. Chatter mechanisms

From the very beginning, metal cutting has had one troublesome obstacle in increasing productivity and accuracy, namely chatter. In machining, chatter is perceived as unwanted excessive vibration between the tool and the workpiece, resulting in a poor surface finish and accelerated tool wear. It also has a deteriorating effect on the machine tool life, and the reliability and safety of the machining operation. The first attempts to describe chatter were made by Arnold (1946), Hahn (1953) and Doi & Kato (1956); however, a comprehensive mathematical model and analysis was given by Tobias & Fishwick (1958). In general, chatter can be classified as primary and secondary. Another classification distinguishes frictional, regenerative, mode-coupling and thermo-mechanical chatter.

Chatter is one of the most common limitations for productivity and part quality in milling operations. Especially for the cases where long slender end mills or highly flexible thin-wall parts, such as air-frame or turbine engine components, are involved, chatter is almost unavoidable unless special suppression techniques are used or the material removal rate is reduced substantially. The importance of modelling and predicting stability in milling has further increased within the last couple of decades, due to the advances in high-speed milling technology (Tlusty 1986). At high speeds, the stabilizing effect of process damping diminishes, making the process more prone to chatter. On the other hand, high stability limits, usually referred to as stability lobes, exist at certain high spindle speeds, which can be used to substantially increase the chatter-free material removal rate, provided that they are predicted accurately (Smith & Tlusty 1993). As a result, chatter-stability analysis continues to be a major topic for machining research. The first accurate modelling of self-excited vibrations in orthogonal cutting was performed by Tlusty & Polacek (1963), Tobias & Fishwick (1958) and Tobias (1965). They identified the most powerful source of self-excitation and regeneration, which are associated with the structural dynamics of the machine tool and the feedback between the subsequent cuts on the same cutting surface. These and other fundamental studies (Merritt 1965) are applicable to orthogonal cutting, where the direction of the cutting force, chip thickness and system dynamics do not change with time. On the other hand, the stability analysis of milling is complicated due to the rotating tool, multiple cutting teeth, periodical cutting forces and chip load directions, and multi-degree-of-freedom structural dynamics. According to Cook (1959), in a typical metal-cutting operation, three processes occur simultaneously:
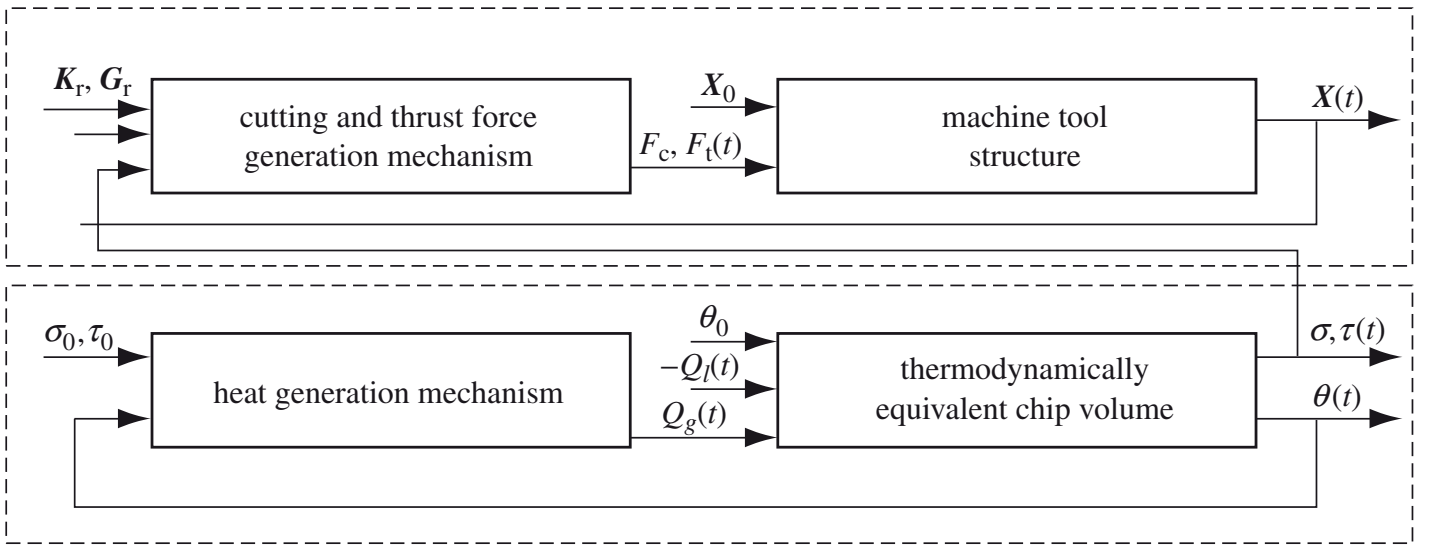
Figure 8. Closed-loop model of dynamic and thermodynamic interaction in the metal-cutting system.

shearing; sliding between chip and tool face; and sliding between workpiece and tool flank. In addition, there is a regeneration effect caused by a variable chip thickness, and each of these processes can be responsible for chatter generation. As mentioned earlier, there are also four different mechanisms of machining chatter: variable friction; regeneration; mode coupling; and thermo-mechanics of chip formation. These mechanisms are interdependent and can generate different types of chatter simultaneously; however, there is not an unified model capable explaining all phenomena observed in machining practice. Therefore, in this section, all important nonlinearities will be spelled out and a systematic review of the main chatter mechanisms will be given.

(a) Nonlinearities in metal cutting

As has been indicated in the previous sections, the metal-cutting process involves a number of strongly nonlinear phenomena, which can be classified into two distinct dynamical systems, namely mechanics and thermodynamics of chip formation. Functional interrelationships between these two systems are shown in figure 8 in a form of a closed-loop model. The idea of portraying the dynamic interactions in the metal cutting as a system of automatic control originated from the work of Merritt (1965), Kegg (1965) and Kudinov (1967). However, all three have only looked at the mechanical part of the problem, and assumed linear dynamics. Grabec (1988), Lin & Weng (1991) and Wiercigroch (1994, 1997) considered mechanical models with nonlinear cutting forces. The model proposed in this paper consists of two inseparable subsystems: mechanical and thermodynamical. The mechanical part is comprised of two major blocks: the cutting and thrust force generation mechanism (CTFGM) and the machine-tool structure (MTS). The inputs to the CTFGM are the required geometry, G_r, and kinematics, K_r, a feedback from the MTS in a form of the dynamical vector $\boldsymbol{X}(t)$, and a feedback from the thermodynamically equivalent chip volume (TECV) in the form of the shear flow stress, $\sigma_s(t)$, and the friction and shear angles, $\tau(t)$ and $\phi(t)$. The outputs from the CTFGM are the cutting and thrust forces, $F_c(t)$ and $F_t(t)$, which, together with the vector of initial conditions, $\boldsymbol{X}_0(t)$, act on the MTS, producing the dynamic vector of displacements and velocities, $\boldsymbol{X}(t)$. The thermo-

dynamical part also consists of two blocks: the heat-generation mechanism (HGM); and, as introduced above, the thermodynamically equivalent chip volume. The HGM is fed with the initial values of $\sigma_{\rm s}(0)$, $\tau(0)$ and $\phi(0)$, and a feedback path of current temperature of the chip, $\theta(t)$.

The system depicted in figure 8 can accommodate all sorts of nonlinearities, in particular, strain hardening and softening (Hastings *et al.* 1980), thermal softening (Davies *et al.* 1997), strain-rate dependence (Oxley 1963), variable friction (Wiercigroch 1997), heat generation and conduction, feed drive hysteresis, intermittent tool engagement (Tlusty & Ismail 1981), structural and contact stiffness in the MTS (Hanna & Tobias 1969), and time delay (Stépán 1998). As an example, a model combining the structural nonlinearities and time delay, proposed by Hanna & Tobias (1974) and thoroughly investigated by Nayfeh *et al.* (1997), is given below

$$\ddot{\hat{x}} + 2\xi\dot{\hat{x}} + \omega_0{}^2(\hat{x} + \beta_{1\rm s}\hat{x}^2 + \beta_{2\rm s}\hat{x}^3) = -\omega_0{}^2[\hat{x} - \hat{x}_T + \beta_{1p}(\hat{x} - \hat{x}_T)^2 + \beta_{2p}(\hat{x} - \hat{x}_T)^3], \quad (3.1)$$

where $\hat{x}_T = \hat{x}(t - T)$. Here, $\hat{x}$ is the non-dimensionalized relative displacement between the cutting tool and the workpiece, ξ the viscous damping of the MTS, ω_0 the fundamental natural frequency, $\beta_{1\rm s}$ and $\beta_{2\rm s}$ are nonlinear stiffness constants, β_{1p} and β_{2p} are nonlinear cutting constants, and T is the time delay, which means a period of one revolution.

(b) Frictional chatter

The effects of the frictional vibration between the tool flank and workpiece has been studied in detail by Cook (1959, 1966), Kegg (1965) and Bailey (1975), and can be elegantly summarized, after Cook (1966), as when rubbing on the clearance face excites vibration in the direction of the cutting force and limits in the thrust force direction. Marui *et al.* (1988a–c) compared the size and orientation of the vibratory locus (trajectory of the cutting edge) for the primary (frictional) and secondary (regenerative) chatters. The distinction between them can be made easily, as the regenerative locus is approximately ten times bigger than the frictional locus and also as their spatial orientations are different. The analytical and experimental studies on the primary chatter reveal that the excitation energy is generated from the friction force both between the workpiece and tool flank and between the chip and the rake surface (e.g. Hamdan & Bayoumi 1989). The friction force on the tool face is generally considered to be the force required to shear the welds formed between the sliding surfaces. Knowing that shear stress varies with the temperature and the shear rate, one can estimate the friction force dependence on the cutting velocity, $v_{\rm c}$. By analysing results presented by Cook (1959), it is apparent that the shear flow stress and the friction force decrease with an increase of chip velocity. Therefore, if there are relative oscillations between the cutting tool and the chip, there will be a net energy input to the system, which can sustain the vibration. A straightforward analysis of a simple one-degree-of-freedom system (Wiercigroch & Krivtsov, this issue) gives conditions for the self-excited vibration (frictional chatter). The amount of viscous damping in the system determines the amplitude of the oscillations. A very strong damping effect can be generated if the vibration velocity exceeds the cutting speed. This is caused by an intermittent contact between the tool and the workpiece (see Wiercigroch (1995, 1997) and Wiercigroch & Cheng (1997) as examples), i.e. the tool is in contact with the chip during a part of the cycle.

(c) Regenerative chatter

The most common form of self-induced vibration is regenerative chatter. It occurs so often because the majority of cutting operations involve overlapping cuts and, although the MTS is stable itself, the amplitude of the forced vibrations resulting from shaving a wavy surface from the previous cut can be significantly amplified (Boothroyd 1975). The experimental work by Kaneko *et al.* (1984) and Marui *et al.* (1988a) provides clear evidence of how dominating the regenerative effect can be when compared with other types of chatter. Kudinov (1955), in his work on the dynamic characteristics of the cutting process, experimentally observed that the cutting force is a function of the depth of cut, and the rake, α, and clearance, β, angles, which can be written as

$$F_c = F_c(h, \alpha, \beta). \tag{3.2}$$

Assuming that this function has a total differential, he proposed a formula for the dynamic variation of the cutting force in the following form:

$$\mathrm{d}F_c = \frac{\partial F_c}{\partial h}\,\mathrm{d}h + \frac{\partial F_c}{\partial \alpha}\,\mathrm{d}\alpha + \frac{\partial F_c}{\partial \beta}\,\mathrm{d}\beta. \tag{3.3}$$

A similar approach of modelling the dynamic variation of the cutting force was adopted in the famous paper by Tobias & Fishwick (1958), where the cutting force in turning was assumed to be a function of the depth of cut, h, the feed rate, r, and the rotational speed, Ω, representing the cutting speed, v_c. The dynamic variation was given as

$$\mathrm{d}F_c = \frac{\partial F_c}{\partial h}\,\mathrm{d}h + \frac{\partial F_c}{\partial r}\,\mathrm{d}r + \frac{\partial F_c}{\partial \Omega}\,\mathrm{d}\Omega, \tag{3.4}$$

where the chip-thickness variation was calculated from

$$\mathrm{d}h = x(t) - \mu x(t - T). \tag{3.5}$$

Here, μ is the factor of overlapping between the previous and present cuts, and T is a period of one revolution. For the first time, the stability of a simple two-degree-of-freedom system excited by a cutting process was elegantly formulated and rigorously analysed. The threshold of stability is described by a set of transcendental equations,

$$1 - \frac{\omega^2}{\omega_0} + \frac{k_1}{k}\left(1 - \mu\cos\frac{2\pi\omega}{\Omega}\right) = 0, \tag{3.6}$$

$$\xi + \mu\frac{k_1}{k}\frac{\omega_0}{\Omega}\sin\frac{2\pi\omega}{\Omega} + \frac{4\pi k_2}{k}\frac{\omega_0}{\Omega} + \frac{2k_3}{k}\frac{\omega_0}{R} = 0, \tag{3.7}$$

where k_1, k_2 and k_3 are machining conditions (Tobias & Fishwick 1958) and R is the instantaneous workpiece radius. Equations (3.6) and (3.7) are used to construct the regenerative stability charts. The nonlinear regenerative-chatter-caused delay has been most recently discussed by Stépán (1998, this issue) and Kalmar-Nagy *et al.* (2001).

(d) Mode coupling

The mode-coupling type of chatter exists if vibration in the thrust force direction generates vibration in the cutting force direction and vice versa. This results
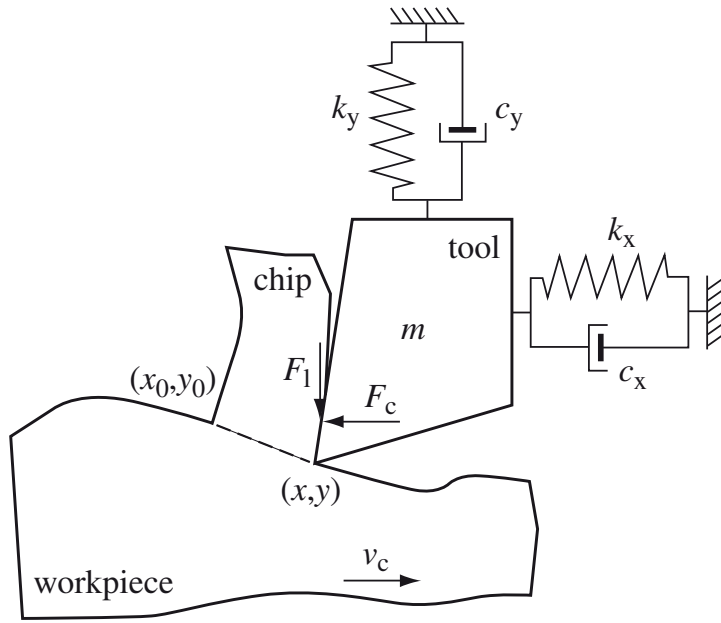
Figure 9. Two-degree-of-freedom model of the metal-cutting system.

in simultaneous vibration in the cutting and thrust force directions. Physically, it is caused by a number of sources, such as friction on the rake and clearance surfaces, as has been explained by Cook (1959) and mathematically described by Wiercigroch (1997), chip-thickness variation (Tlusty & Ismail 1981), shear angle oscillations (Knight 1970; Wu 1986), and regeneration effect (Jemielniak & Widota 1988; Altinitas & Budak 1995). The necessary condition is that the cutting and thrust forces have components (feedback) of other directions. This has been elegantly captured for a two-degree-of-freedom model by Wu & Liu (1985a) (as shown in figure 9) in the form of two expressions for the cutting and thrust forces,

$$m\ddot{x} + c_x\dot{x} + k_x x = 2w\sigma_s(x_0 - x)[(A_x - C_x v_0)$$
$$+ \tfrac{1}{2}B_x(\dot{x} - \dot{x_0}) - \tfrac{1}{2}C_x(\dot{y} - \dot{y_0})] - \frac{Kw}{v_c}\dot{x}, \quad (3.8)$$

$$m\ddot{y} + c_y\dot{y} + k_y y = 2w\sigma_s(x_0 - x)[(A_y - C_y v_c) + \tfrac{1}{2}B_y(\dot{x} - \dot{x_0}) - \tfrac{1}{2}C_y(\dot{y} - \dot{y_0})], \quad (3.9)$$

where m is the equivalent vibrating mass, c_x and c_y the viscous damping coefficients, k_x and k_y the machine structure stiffness constants, v_c the cutting speed, and K is the damping coefficient evaluated from the ploughing force acting on the tool nose (see, for example, Moriwaki & Narutaki 1969; Kegg 1969). The remaining constants in (3.8) and (3.9) (A_x, A_y, B_x, B_y, C_x and C_y) are called the dynamic force coefficients and are fully described in Wu & Liu (1985a).

(e) Thermomechanical chatter

The first approach to comprehensively describe the thermomechanics was made by Hastings *et al.* (1980), where an approximate machining theory was formulated to account for the effects of temperature and strain-rate in the plastic deformation zone on the overall mechanics of chip formation. The theory was applied to two plain carbon steels by using the flow stress data obtained from high-speed cutting (high-speed compression rates), and a good agreement between theory and experiment has been shown for predicting the cutting and thrust forces. The approach is based on the so-called tool-chip plastic zone thickness, predicted from a minimum work criterion, which is central to explain an experimentally observed decrease in chip

thickness with an increase in cutting speed. The mathematical model outlined in the previous section can be used to generate velocity-dependent chatter (see Grabec 1988); however, it fails to explain formation of segmented chips. As mentioned earlier, Recht (1985) came up with an interesting hypothesis, where all important stages of the segmented chip formation are explained descriptively. The first real mathematical justification explaining the mechanism of segmented chips formation was proposed by Davies *et al.* (1997), where a simplified one-dimensional thermomechanical model of a continuous homogeneous material being sheared by a rigid tool was used. In this model, the following main assumptions have been made.

(i) The workpiece is in a form of a continuous one-dimensional slab with thermal softening and strain-rate hardening.

(ii) Interactions between the workpiece and the tool obey local elasto-plastic strain–stress laws.

(iii) Only stresses parallel to the shear plane are considered.

(iv) The momentum of the chip is ignored.

(v) The tool is rigid and non-conductive.

(vi) The specific heat, conductivity and density of the workpiece are constant.

By considering the stress and heat transfer equilibria of a discretized model (Davies *et al.* 1997), a mathematical model in the form of a set of three partial differential equations and one ordinary differential equation has been derived. Numerical simulations of this model shows that, as cutting speed is increased, a transition from continuous to shear-localized chip formation takes place, with an initial, somehow disordered, phase. Increasing cutting speed further, the average spacing between shear bands becomes more regular, asymptotically approaching a limit value, as was observed in experimental studies.

4. Case study: chatter elimination in the milling process

(a) Background

In the early milling stability analysis, Koenigsberger & Tlusty (1967) used their orthogonal cutting model to consider an average direction and average number of teeth in cut. An improved approximation was performed by Opitz & Bernardi (1970). Later, however, Tlusty & Ismail (1981) showed that the time-domain simulations would be required for accurate stability predictions in milling. Sridhar *et al.* (1968*a*, *b*) performed a comprehensive analysis of milling stability, which involved numerical evaluation of the dynamic milling system state transition matrix. On a two-degree-of-freedom cutter model with point contact, Minis *et al.* (1990) and Minis & Yanushevsky (1993) used Floquet's theorem and the Fourier series (Magnus & Winkler 1966) for the formulation of the milling stability, and numerically solved it using the Nyquist criterion. Budak (1994) developed a stability method, which leads to an analytical determination of stability limits. The method was verified by experimental and numerical means, and was demonstrated to be effective for the generation of stability lobe diagrams (Budak & Altintas 1998). This method was also applied to

the stability of ball-end milling by Altintas *et al.* (1999*b*). Another method of chatter suppression in milling is the application of cutting tools with irregular spacing, or variable pitch cutters. The basic idea behind these cutters is to eliminate or reduce regeneration in chip thickness by altering the phase between successive vibration waves on the cutting surface. Variable pitch cutters are particularly useful in cases where high-stability lobes cannot be used due to speed limitations for the machine or work material (Budak & Kops 2000).

The effectiveness of variable pitch cutters in suppressing chatter vibrations in milling was first demonstrated by Slavicek (1965). He assumed a rectilinear tool motion for the cutting teeth and applied the orthogonal stability theory to irregular tooth pitch. By assuming an alternating pitch variation, he obtained a stability-limit expression as a function of the variation in the pitch. Opitz (1968) considered milling tool rotation using average directional factors. They also considered alternating pitch with only two different pitch angles. Their experimental results and predictions showed significant increases in the stability limit using cutters with alternating pitch. Another significant study on these cutters was performed by Vanherck (1967), who considered different pitch variation patterns in the analysis by assuming rectilinear tool motion. His detailed computer simulations showed the effect of pitch variation on stability limit. Later, Tlusty *et al.* (1983) analysed the stability of milling cutters, with special geometries such as irregular pitch and serrated edges, using numerical simulations. Their results confirmed the previous observations that, for a certain pitch variation, high improvements in stability can be achieved only for limited speed and chatter frequency ranges. Altintas *et al.* (1999*a*) adopted the analytical milling stability model to the case of variable pitch cutters, which can be used to predict the stability with variable pitch cutters accurately. Recently, Budak & Kops (2000) developed an analytical method for the optimal design of pitch angles in order to maximize stability limit. In this section, the analytical chatter-stability method presented by Budak & Altintas (1998) will be summarized. The original model considers the dynamic interaction between tool and workpiece, including variation in dynamics and mode shapes along the axial direction. This introduces a non-linearity to the system, as the system dynamics, and thus the characteristic equation, depend on the depth of the cut, which is the sought after solution. The details of this solution can be found in Budak (1994) and Budak & Altintas (1998) and will not be considered here. Instead, a case of simple point contact will be analysed. The extension of the method to variable pitch-cutter stability will also be presented. Application of the models will be demonstrated through numerical and experimental examples.

(b) Stability of milling for regular cutters

In this analysis, both milling cutter and workpiece are considered to have two orthogonal modal directions, as shown in figure 10.

Milling forces excite both cutter and workpiece, causing vibrations, which are imprinted on the cutting surface. Each vibrating cutting tooth removes the wavy surface left from the previous tooth, resulting in modulated chip thickness which can be expressed as follows,

$$h_j(\phi) = s_{\mathrm{t}} \sin \phi_j + (v_{j_{\mathrm{c}}}^0 - v_{j_{\mathrm{w}}}^0) - (v_{j_{\mathrm{c}}} - v_{j_{\mathrm{w}}}), \tag{4.1}$$
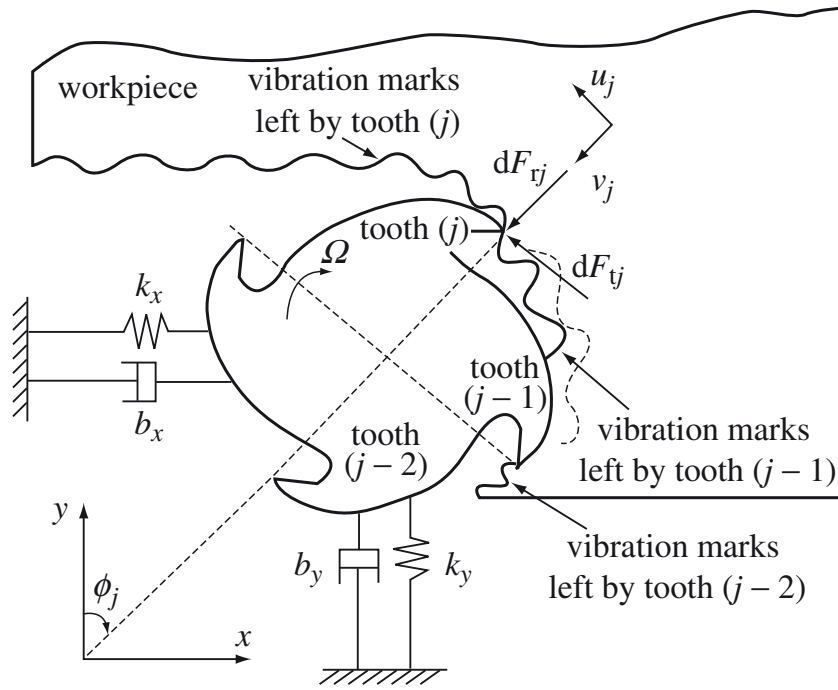
Figure 10. Dynamic model of milling.

where the feed per tooth, s_t represents the static part of the chip thickness, and $\phi_j = (j-1)\phi_p + \phi$ is the angular immersion of tooth j for a cutter with constant pitch angle $\phi_p = 2\pi/N$ and N teeth, as shown in figure 10. $\phi = \Omega t$ is the angular position of the cutter, measured with respect to the first tooth and corresponding to the rotational speed Ω (rad s^{-1}). v_j and v_j^0 are the dynamic displacements due to tool and workpiece vibrations for the current and previous tooth passes, for the angular position ϕ_j, and can be expressed in terms of the fixed coordinate system as

$$v_{j_p} = -x_p \sin\phi_j - y_p \cos\phi_j \qquad (p = \mathrm{c}, \mathrm{w}), \qquad (4.2)$$

where 'w' and 'c' indicate workpiece and cutter, respectively. The static part in (4.1), $s_t \sin\phi_j$, is neglected in the stability analysis. It should be noted that even though the static chip thickness varies in time as the milling cutter rotates, it does not contribute to regeneration, and thus can be eliminated in chatter-stability analysis. However, it should also be noted that the static chip thickness is of importance for nonlinear stability analysis, as it determines when the contact between the cutting tooth and the material is lost due to vibrations. Since we are interested in determining the stability limit, where the system is still stable and the contact between the cutter and the chip is not lost, this nonlinearity will not be considered. If (4.2) is substituted in (4.1), the following expression is obtained for the dynamic chip thickness in milling,

$$h_j(\phi) = [\Delta x \sin\phi_j + \Delta y \cos\phi_j], \qquad (4.3)$$

where

$$\left.\begin{array}{l} \Delta x = (x_\mathrm{c} - x_\mathrm{c}^0) - (x_\mathrm{w} - x_\mathrm{w}^0), \\ \Delta y = (y_\mathrm{c} - y_\mathrm{c}^0) - (y_\mathrm{w} - y_\mathrm{w}^0), \end{array}\right\} \qquad (4.4)$$

in which $(x_\mathrm{c}, y_\mathrm{c})$ and $(x_\mathrm{w}, y_\mathrm{w})$ are the dynamic displacements of the cutter and the workpiece in the x- and y-directions, respectively. The dynamic cutting forces on tooth j in the tangential and the radial directions can be expressed as follows,

$$F_{\mathrm{t}_j}(\phi) = K_\mathrm{t} a h_j(\phi), \qquad F_{\mathrm{r}_j} = K_\mathrm{r} F_{\mathrm{t}_j}(\phi), \qquad (4.5)$$

where a is the axial depth of cut and K_t and K_r are the cutting force coefficients which are experimentally identified (Armarego & Whitfield 1985; Budak *et al.* 1996). After substituting h_j from (4.1) into (4.5) and summing up the forces on each tooth ($F = \sum F_j$), the dynamic milling forces can be resolved in the x- and y-directions as

$$\begin{Bmatrix} F_x \\ F_y \end{Bmatrix} = \tfrac{1}{2} a K_t \begin{bmatrix} a_{xx} & a_{xy} \\ a_{yx} & a_{yy} \end{bmatrix} \begin{Bmatrix} \Delta x \\ \Delta y \end{Bmatrix}, \tag{4.6}$$

where the directional coefficients are given as

$$\left. \begin{aligned} a_{xx} &= - \sum_{j=1}^{N} \sin 2\phi_j + K_r (1 - \cos 2\phi_j), \\ a_{xy} &= - \sum_{j=1}^{N} (1 + \cos 2\phi_j) + K_r \sin 2\phi_j, \\ a_{yx} &= - \sum_{j=1}^{N} -(1 - \cos 2\phi_j) + K_r \sin 2\phi_j, \\ a_{yy} &= - \sum_{j=1}^{N} - \sin 2\phi_j + K_r (1 + \cos 2\phi_j). \end{aligned} \right\} \tag{4.7}$$

The directional coefficients depend on the angular position of the cutter, which makes (4.6) time-varying,

$$\{F(t)\} = \tfrac{1}{2} a K_t [A(t)] \{\Delta(t)\}, \tag{4.8}$$

in which the matrix $[A(t)]$ is the periodic function at the tooth-passing frequency $\omega = N\Omega$ and with corresponding period of $T = 2\pi/\omega$. In general, the Fourier series expansion of the periodic term is used for the solution of the periodic systems (Magnus & Winkler 1966). The solution can be obtained numerically by truncating the resulting infinite determinant. However, in chatter-stability analysis, inclusion of the higher harmonics in the solution may not be required, as the response at the chatter limit is usually dominated by a single chatter frequency. Starting from this idea, Altintas & Budak (1995) have shown that the higher harmonics do not affect the accuracy of the predictions, and it is sufficient to include only the average term in the Fourier series expansion of $[A(t)]$,

$$[A_0] = \frac{1}{T} \int_0^T [A(t)] \, \mathrm{d}t. \tag{4.9}$$

As all the terms in $[A(t)]$ are valid within the cutting zone between start and exit immersion angles (ϕ_{st}, ϕ_{ex}), equation (4.9) reduces to the following form in the angular domain,

$$[A_0] = \frac{1}{\phi_p} \int_{\phi_{st}}^{\phi_{ex}} [A(\phi)] \, \mathrm{d}\phi = \frac{N}{2\pi} \begin{bmatrix} \alpha_{xx} & \alpha_{xy} \\ \alpha_{yx} & \alpha_{yy} \end{bmatrix}, \tag{4.10}$$

where the integrated, or average, directional coefficients are given as

$$
\left.\begin{aligned}
\alpha_{xx} &= \tfrac{1}{2}[\cos 2\phi - 2K_\mathrm{r}\phi + K_\mathrm{r}\sin 2\phi]_{\phi_\mathrm{st}}^{\phi_\mathrm{ex}}, \\
\alpha_{xy} &= \tfrac{1}{2}[-\sin 2\phi - 2\phi + K_\mathrm{r}\cos 2\phi]_{\phi_\mathrm{st}}^{\phi_\mathrm{ex}}, \\
\alpha_{yx} &= \tfrac{1}{2}[-\sin 2\phi + 2\phi + K_\mathrm{r}\cos 2\phi]_{\phi_\mathrm{st}}^{\phi_\mathrm{ex}}, \\
\alpha_{xx} &= \tfrac{1}{2}[-\cos 2\phi - 2K_\mathrm{r}\phi - K_\mathrm{r}\sin 2\phi]_{\phi_\mathrm{st}}^{\phi_\mathrm{ex}}.
\end{aligned}\right\}
\tag{4.11}
$$

Substituting (4.11), equation (4.8) reduces to the following form:

$$
\{F(t)\} = \tfrac{1}{2}aK_\mathrm{t}[A_0]\{\Delta(t)\}.
\tag{4.12}
$$

Chatter-stability limit

The dynamic displacement vector in (4.12) can be described as

$$
\{\Delta(t)\} = (\{r_\mathrm{c}\} - \{r_\mathrm{c}^0\}) - (\{r_\mathrm{w}\} - \{r_\mathrm{w}^0\}),
\tag{4.13}
$$

where

$$
\{r_p\} = [\{x_p\}\{y_p\}]^T \qquad (p = \mathrm{c}, \mathrm{w}).
\tag{4.14}
$$

The response of both structures at the chatter frequency can be expressed as follows,

$$
\{r_p(\mathrm{i}\omega_\mathrm{c})\} = [G_p(\mathrm{i}\omega_\mathrm{c})]\{F\}\mathrm{e}^{-\mathrm{i}\omega_\mathrm{c}t} \qquad (p = \mathrm{c}, \mathrm{w}),
\tag{4.15}
$$

where F represents the amplitude of the dynamic milling force $F(t)$, and the transfer function matrix is given as

$$
[G_p] = \begin{bmatrix} G_{p_{xx}} & G_{p_{xy}} \\ G_{p_{yx}} & G_{p_{yy}} \end{bmatrix} \qquad (p = \mathrm{c}, \mathrm{w}).
\tag{4.16}
$$

The vibrations at the previous tooth period, i.e. at $t - T$, can be defined as follows:

$$
\left.\begin{aligned}
\{r_p^0\} &= [\{x_p(t - T)\}\{y_p(t - T)\}]^T, \\
\{r_p^0\} &= \mathrm{e}^{-\mathrm{i}\omega_\mathrm{c}T}\{r_p\},
\end{aligned}\right\} \qquad (p = \mathrm{c}, \mathrm{w}).
\tag{4.17}
$$

By substituting (4.13)–(4.17) into the dynamic milling force expression given in (4.12), the following is obtained,

$$
\{F\}\mathrm{e}^{\mathrm{i}\omega_\mathrm{c}t} = \tfrac{1}{2}aK_\mathrm{t}(1 - \mathrm{e}^{-\mathrm{i}\omega_\mathrm{c}T})[A_0][G(\mathrm{i}\omega_\mathrm{c})]\{F\}\mathrm{e}^{\mathrm{i}\omega_\mathrm{c}t},
\tag{4.18}
$$

where

$$
[G(\mathrm{i}\omega_\mathrm{c})] = [G_\mathrm{c}(\mathrm{i}\omega_\mathrm{c})] + [G_\mathrm{w}(\mathrm{i}\omega_\mathrm{c})]
\tag{4.19}
$$

has a non-trivial solution only if its determinant is zero,

$$
\det[[I] + \Lambda[G_0(\mathrm{i}\omega_\mathrm{c})]] = 0,
\tag{4.20}
$$

where $[I]$ is the unit matrix and the oriented transfer function matrix is defined as

$$
[G_0] = [A_0][G],
\tag{4.21}
$$

and the eigenvalue Λ in (4.20) is given as

$$
\Lambda = -\frac{N}{4\pi}K_\mathrm{t}a(1 - \mathrm{e}^{-\mathrm{i}\omega_\mathrm{c}T}).
\tag{4.22}
$$

If the eigenvalue Λ is known, the stability limit can be determined from (4.22). Λ can easily be computed numerically from (4.20). However, an analytical solution is possible if the cross transfer functions, G_{xy} and G_{yx}, are neglected in (4.20),

$$\Lambda = -\frac{1}{2a_0}\left(a_1 \pm \sqrt{a_1^2 - 4a_0}\right), \tag{4.23}$$

where

$$\left.\begin{aligned} a_0 &= G_{xx}(\mathrm{i}\omega_\mathrm{c})G_{yy}(\mathrm{i}\omega_\mathrm{c})(\alpha_{xx}\alpha_{yy} - \alpha_{xy}\alpha_{yx}), \\ a_1 &= \alpha_{xx}G_{xx}(\mathrm{i}\omega_\mathrm{c}) + \alpha_{yy}G_{yy}(\mathrm{i}\omega_\mathrm{c}). \end{aligned}\right\} \tag{4.24}$$

This is a valid assumption for the majority of the milling systems, i.e. the cross transfer functions are negligible, such as slender end mills and plate-like workpieces.

Since the transfer functions are complex, Λ will have complex and real parts. However, the axial depth of cut a is a real number. Therefore, when $\Lambda = \Lambda_\mathrm{R} + \mathrm{i}\Lambda_\mathrm{I}$ and $\mathrm{e}^{-\mathrm{i}\omega_\mathrm{c}T} = \cos\omega_\mathrm{c}T - \mathrm{i}\sin\omega_\mathrm{c}T$ are substituted in (4.22), the complex part of the equation has to vanish, yielding

$$\kappa = \frac{\Lambda_\mathrm{I}}{\Lambda_\mathrm{R}} = \frac{\sin\omega_\mathrm{c}T}{1 - \cos\omega_\mathrm{c}T}. \tag{4.25}$$

The above can be solved to obtain a relation between the chatter frequency and the spindle speed (Altintas & Budak 1995; Budak & Altintas 1998),

$$\left.\begin{aligned} \omega_\mathrm{c}T &= \varepsilon + 2k\pi, \\ \varepsilon &= \pi - 2\psi, \\ \psi &= \tan^{-1}\kappa, \\ n &= 60/(NT), \end{aligned}\right\} \tag{4.26}$$

where ε is the phase difference between the inner and outer modulations, k is an integer corresponding to the number of vibration waves within a tooth period, and n is the spindle speed (RPM). After the imaginary part in (4.22) vanishes, the following is obtained for the stability limit (Altintas & Budak 1995; Budak & Altintas 1998):

$$a_\mathrm{lim} = \frac{2\pi\Lambda_\mathrm{R}}{NK_\mathrm{t}}(1 + \kappa^2). \tag{4.27}$$

Therefore, for given cutting geometry, cutting-force coefficients, tool and workpiece transfer functions and chatter frequency ω_c, Λ_I and Λ_R can be determined from (4.23), and can be used in (4.26) and (4.27) to determine the corresponding spindle speed and stability limit. When this procedure is repeated for a range of chatter frequencies and number of vibration waves, k, the stability lobe diagram for a milling system is obtained.

Example 4.1. Demonstration of the method will be done on a two-degree-of-freedom end-milling example given in Budak & Altintas (1998). The dynamic properties of the 3-flute end mill in two orthogonal directions were identified in Weck *et al.* (1994), and are given in table 1.

The aluminium workpiece is considered to be rigid compared with the cutter. The experimental stability limits (Weck *et al.* 1994) and simulations for a half-immersion (up-milling) case are shown in figure 11. As can be seen from this figure,
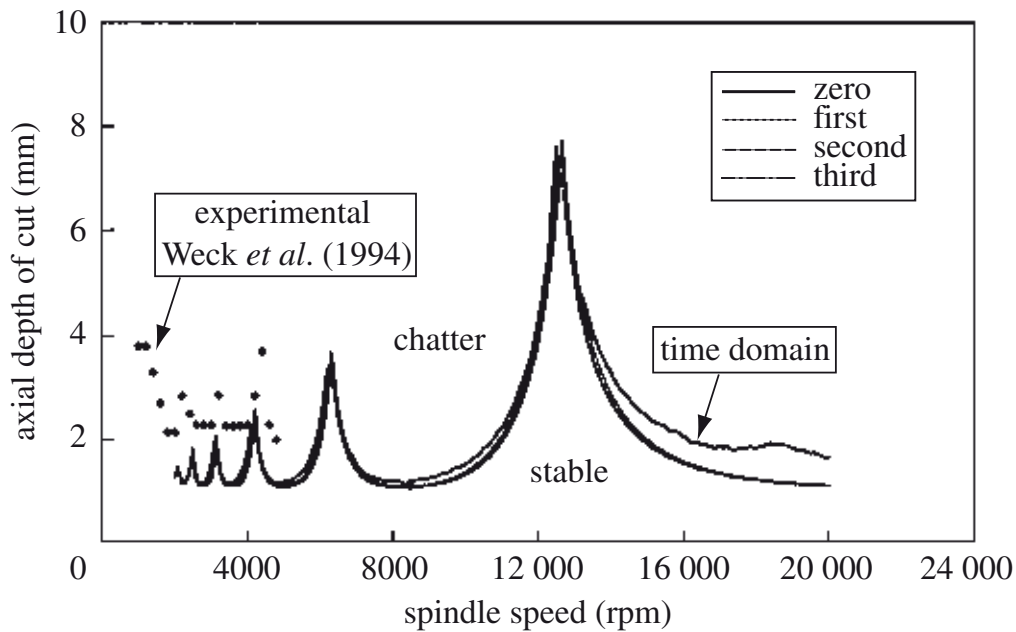
Figure 11. Analytical and experimental stability diagrams for a two-degree-of-freedom milling system considered in the example.

Table 1. *Dynamics properties of 3-flute end mill*

	ω_c (Hz)	k (kH m^{-1})	ζ
X	603	5600	0.039
Y	666	5700	0.035

the stability-limit predictions using zero- or higher-order approximations are very close. Furthermore, there is a very good agreement between the numerical time-domain solution and the analytical predictions. It should be noted that the analytical stability diagram can be generated in a few seconds, whereas time-domain simulations usually take several hours (up to a full day), depending on the precision required. In time-domain simulations, dynamic system equations have to be simulated over several tool rotations using very small time-steps.

(c) Stability of milling for cutters with non-constant pitch

The fundamental difference in the stability analysis of milling cutters with non-constant pitch angle is that the phase delay between the inner and the outer waves is different for each tooth and can described as

$$\varepsilon_j = \omega_c T_j \qquad (j = 1, \ldots, N),\tag{4.28}$$

where T_j is the jth tooth period corresponding to the pitch angle ϕ_{pj}. The dynamic variation of chip thickness and the cutting force relations given for the standard milling cutters apply to the variable pitch cutters as well. The directional coefficients given in (4.10) are evaluated at the average pitch angle to simplify the formulation. Then the characteristic equation given in (4.22) is valid for the variable pitch cutters; however, the eigenvalue expression will take the following form due to the varying phase:

$$\Lambda = \frac{a}{4\pi} K_t \sum_{j=1}^{N} (1 - e^{-i\omega_c T_j}).\tag{4.29}$$

22

The stability limit can be obtained from (4.29) as

$$a_{\text{lim}}^{\text{vp}} = -\frac{4\pi}{K_t} \frac{\Lambda}{N - C + iS}, \tag{4.30}$$

where

$$\left.\begin{aligned} C &= \sum_{j=1}^{N} \cos \omega_c T_j, \\ S &= \sum_{j=1}^{N} \sin \omega_c T_j. \end{aligned}\right\} \tag{4.31}$$

Since the eigenvalue is a complex number, if $\Lambda = \Lambda_R + \Lambda_I$ is substituted in (4.30), the following formula is obtained:

$$a_{\text{lim}}^{\text{vp}} = -\frac{4\pi}{K_t} \left[\frac{(N - C)\Lambda_R + S\Lambda_I}{(N - C)^2 + S^2} + i\frac{(N - C)\Lambda_I - S\Lambda_R}{(N - C)^2 + S^2} \right]. \tag{4.32}$$

As a_{lim} is a real number, the imaginary part of (4.32) must vanish, therefore,

$$N - C = S\frac{\Lambda_R}{\Lambda_I}. \tag{4.33}$$

By substituting the above expression into (4.32), a_{lim} simplifies to

$$a_{\text{lim}}^{\text{vp}} = -\frac{4\pi}{K_t} \frac{\Lambda_I}{S}. \tag{4.34}$$

It is interesting to note that the stability limit obtained for the equal pitch cutters (equation (4.27)) can be put into a similar form by substituting κ from (4.25),

$$a_{\text{lim}}^{\text{vp}} = -\frac{4\pi}{K_t} \frac{\Lambda_I}{N \sin \omega_c T}. \tag{4.35}$$

Note that for equal pitch cutters, $S = \sum \sin \omega_c T$ in (4.34) becomes $N \sin \omega_c T$ in (4.35), as the phase ($\omega_c T$) is the same for all the teeth. The stability limit with variable pitch cutters can be determined using (4.33) and (4.34). Unlike for the equal-pitch cutters, in this case, the solution has to be determined numerically, since an explicit equation for the chatter-frequency–spindle-speed relation cannot be obtained from (4.33). Also, the cutter pitch angles have to be known in advance. However, optimization of pitch angles for a given milling system has more practical importance than the stability analysis of an arbitrary variable pitch cutter. Therefore, the rest of the analysis focuses on the optimization of the pitch angles to maximize the stability against chatter.

Equation (4.34) indicates that in order to maximize the stability limit, $|S|$ has to be minimized. From (4.31), S can be expressed as follows,

$$S = \sin \varepsilon_1 + \sin \varepsilon_2 + \sin \varepsilon_3 + \cdots, \tag{4.36}$$

where $\varepsilon_j = \omega_c T_j$. The phase angle, which is different for every tooth due to the non-constant pitch, can be expressed as follows,

$$\varepsilon_j = \varepsilon_1 + \Delta\varepsilon_j \qquad (j = 2, N), \tag{4.37}$$

where $\Delta\varepsilon_j$ is the phase difference between tooth j and tooth 1 corresponding to the difference in the pitch angles between these teeth. By considering the number of vibration waves in one cutter revolution, m, we can further develop this relation,

$$m = \frac{\omega_c}{\Omega}, \tag{4.38}$$

where Ω is the spindle speed (rad s^{-1}). Note that m is the summation of the full number of waves and the remaining fraction of a wave, and thus it is, in general, a non-integer number. If θ is defined as the tooth immersion angle corresponding to one full vibration, it is determined as

$$\theta = \frac{2\pi}{m} = \frac{2\pi\Omega}{\omega_c}. \tag{4.39}$$

Therefore, the pitch angle variation ΔP corresponding to $\Delta\varepsilon$ can be determined from

$$\Delta P = \frac{\Delta\varepsilon}{2\pi}\theta = \frac{\Omega}{\omega_c}\Delta\varepsilon. \tag{4.40}$$

Thus ΔP and $\Delta\varepsilon$ are linearly proportional. Using (4.37), equation (4.36) can be expanded as follows:

$$S = \sin\varepsilon_1 + \sin\varepsilon_1\cos\Delta\varepsilon_2 + \sin\Delta\varepsilon_2\cos\varepsilon_1 + \sin\varepsilon_1\cos\Delta\varepsilon_3 + \sin\Delta\varepsilon_3\cos\varepsilon_1 + \cdots. \tag{4.41}$$

There are many solutions for the minimization of $|S|$, i.e. $S = 0$. For example, for an even number of teeth, $S = 0$ when $\Delta\varepsilon_j = j\pi$. This can easily be achieved by using linear or alternating pitch variation,

$$\left.\begin{array}{ll} \text{linear:} & P_0,\ P_0 + \Delta P,\ P_0 + 2\Delta P,\ P_0 + 3\Delta P, \\ \text{alternating:} & P_0,\ P_0 + \Delta P,\ P_0 + \Delta P,\ \ldots. \end{array}\right\} \tag{4.42}$$

A more general solution can be obtained by substituting a specific pitch variation pattern into S. For the linear pitch variation, S takes the following form

$$S = \sin\varepsilon_1(1 + \cos\Delta\varepsilon + \cos 2\Delta\varepsilon + \cdots) + \cos\varepsilon_1(\sin\Delta\varepsilon + \sin 2\Delta\varepsilon + \cdots). \tag{4.43}$$

Intuitively, it can be predicted that, in (4.43), $S = 0$ for the following conditions:

$$\Delta\varepsilon = k\frac{2\pi}{N} \qquad (k = 1, 2, \ldots, N-1). \tag{4.44}$$

The corresponding ΔP can be determined using (4.40). The increase of the stability with variable pitch cutters over the standard end mills can be determined by considering the ratio of stability limits. For simplicity, the absolute or critical stability limit for equal pitch cutters are considered. The absolute stability limit is the minimum stable depth of cut without the effect of lobing, which can be expressed as follows (cf. (4.35)):

$$a_{cr} = -\frac{4\pi\Lambda_I}{NK_t}. \tag{4.45}$$

Then the stability gain can be expressed as

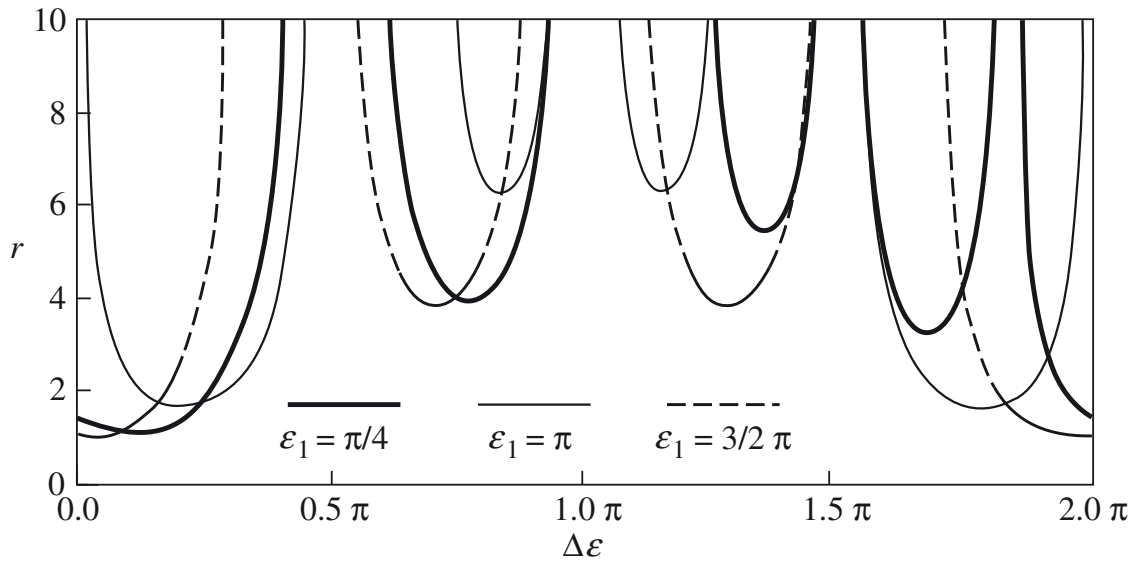$$r = \frac{a_{lim}^{vp}}{a_{cr}} = \frac{N}{S}. \tag{4.46}$$

Figure 12. The effect of $\Delta\varepsilon$ on stability gain for a 4-fluted end mill with linear pitch variation.

r is plotted as a function of $\Delta\varepsilon$ in figure 12 for a 4-tooth milling cutter with linear pitch variation. The phase ε depends on the chatter frequency, spindle speed and the eigenvalue of the characteristic equation, and therefore the stability analysis has to be performed for the given conditions. However, this can only be done for a given cutting tool geometry, i.e. pitch-variation pattern. Therefore, three different curves corresponding to different ε_1 values are shown in figure 12 to demonstrate the effect of phase variation on r. As expected, ε_1 has a strong effect on r and $\frac{3}{2}\pi$ results in the lowest stability gain. Also, as predicted by (4.44), r is maximized for integer multiples of $2\pi/N$, i.e. for $(\frac{1}{4}, \frac{1}{2}, \frac{3}{4}) \times 2\pi$. $\Delta\varepsilon + k2\pi$ $(k = 1, 2, 3, \dots)$ are also optimal solutions. However, they result in higher pitch variations, which are not desired since they increase the variation in the chip load from tooth to tooth. The optimal pitch variation can be determined if the chatter frequency and the spindle speed are known before the cutter is designed. This can be done by simple acoustic measurements using an equal-pitch cutting tool to determine the chatter frequency. The chatter frequency may vary with the introduction of the variable pitch cutter, or be due to the changes in the machine condition, part clamping and workpiece dynamics. Modal analysis of the part–tool–spindle system is usually very useful to determine the other important modes.

As can also be seen from figure 12, for linear pitch variation, a minimum of $r = 4$ gain is obtained for a 4-tooth cutter for $0.5\pi < \Delta\varepsilon < 1.5\pi$. Thus the target for $\Delta\pi$ should be π, which is one of the optimal solutions for the cutters with an even number of flutes, but it is also in the middle of the high-stability area. Other variation types were also tried; however, they gave smaller high-stability gain areas than linear variation. Therefore, the optimal pitch variation can be determined as

$$\Delta P = \begin{cases} \pi \dfrac{\Omega}{\omega_c} & \text{for even } N, \\[2ex] \pi \dfrac{\Omega}{\omega_c} \dfrac{(N \pm 1)}{N} & \text{for odd } N. \end{cases} \qquad (4.47)$$

The pitch angles have to satisfy the following relation:

$$P_0 + (P_0 + \Delta P) + (P_0 + 2\Delta P) + \cdots + [P_0 + (N-1)\Delta P] = 2\pi. \qquad (4.48)$$
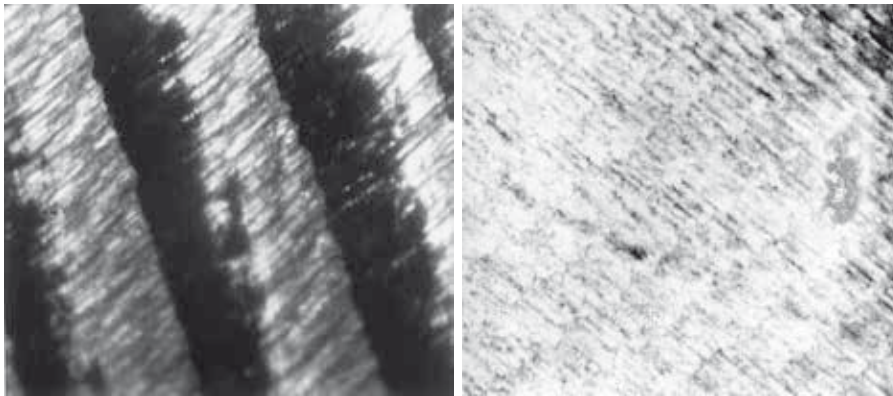
Figure 13. Surface improvement due to variable pitch cutter in example 4.2.

P_0 can be determined from (4.48) as follows:

$$P_0 = \frac{2\pi}{N} - \tfrac{1}{2}(N-1)\Delta P. \qquad (4.49)$$

Example 4.2. In this example, the milling of an airfoil made out of titanium alloy, Ti6Al4V, is considered. The stability limit of the process is extremely small due to the highly flexible workpiece and cutting tool. A 6-fluted carbide taper ball end mill with length-to-average diameter ratio of over 10 is used on a 5-axis machining centre. For one of the finishing passes, the axial depth of cut is over 100 mm. This is very much higher than the stability limit of the process, thus a very low spindle speed is used to maximize process damping. However, even at 300 RPM, severe chatter vibrations are experienced with the equal pitch cutter. For the 420 Hz chatter frequency, $P = 55, 57, 59, 61, 63, 65$ pitch variation is obtained from (4.47) and (4.49) (for 300 RPM). This cutter suppresses the chatter completely. As a result, the surface finish is significantly improved, as shown in figure 13.

5. Synopsis

In this paper a critical review of state-of-the-art modelling and experimental investigations has been presented, with a view to how the nonlinear-dynamics perception could help to capture the major phenomena causing instabilities in machining operations.

In general, the cutting process is a result of the dynamic interactions between the machine tool, the cutting tool and the workpiece. Therefore, its mathematical description should take into account its kinematics, dynamics, geometry of the chip formation, and the workpiece's mechanical and thermodynamical properties. Mechanics of the cutting process and chip formation are being recognized, more now than ever before, as the key issue in the development of machining technologies. The complexity of the cutting process is due to the interwoven physical phenomena such as elasto-plastic deformations in the cutting zones, variable friction between tool and chip and workpiece, heat generation and transfer, adhesion and diffusion, and material structural and phase transformations, to name but a few. An understanding of these relationships is the most important issue in the modelling of the cutting processes, as the majority of the phenomena listed here are strongly nonlinear and interdependent.

Studies on metal-cutting processes were carried out as early as the 1800s. However, only by the mid-1940s and 1950s had two researchers, Piispanen (1937, 1948) and

Merchant (1944, 1945a, b), described the flow of metal chips. Based on this concept of orthogonal cutting, the continuous chip is formed by a cutting process, which was understood to be confined to a single shear plane extending from the cutting edge to the shear plane. The force diagram developed by Merchant (1944) has been used extensively up until now.

The model of *dynamic cutting characteristics* developed by Kudinov (1955, 1963, 1967) has been widely used in the former Soviet Union and Eastern Europe. It assumes that chatter, variation of the cutting and thrust forces are due to variations of chip thickness and relative kinematics between the tool and workpiece. The starting point of his scheme was the cutting force, which was evaluated for steady-state conditions from a semi-empirical formula (Loladze 1952). Then a functional relationship describing the cutting force was established, assuming that it is a total differential. In the original work by Kudinov (1963), the dynamic forces are given in the Laplace space (see (2.22) and (2.23)). This approach was further developed by other Russian researchers such as Abakumov *et al.* (1972) and Zharkov (1985), who have included regenerative effects in the model.

An interesting approach explaining the influence of the temperature and the strain-rate-dependent properties of the workpiece has been given in the paper by Hastings *et al.* (1980), who assumed plane strain and steady-state conditions as in Merchant's model. They proposed a set of analytically empirical equations allowing us, for the first time, to calculate the temperature and the strain rate at the cutting-tool–chip interface, in addition to the expressions for the cutting and thrust forces. The only reservation one should have is the empirical nature of some of the formulae and the fact that the non-monotonic nonlinear relation between the flow stress and the chip temperature is hardly reflected in the cutting/thrust force versus cutting-speed characteristics (see figure 7).

From the very beginning, metal cutting has had one troublesome obstacle in increasing productivity and accuracy, namely chatter. In machining, chatter is perceived as unwanted excessive vibration between the tool and the workpiece, resulting in a poor surface finish. It has also a deteriorating effect on the reliability and safety of this machining operation. The first attempts to describe chatter were made by Arnold (1946), Hahn (1953) and Doi & Kato (1956); a comprehensive mathematical model and analysis was given by Tobias & Fishwick (1958). In general, chatter can be classified as primary and secondary. Another classification distinguishes frictional, regenerative, mode-coupling and thermomechanical chatter. Chatter is one of the most common limitations for productivity and part quality in milling operations. Especially for the cases where long slender end mills or highly flexible thin-wall parts such as air-frame or turbine engine components are involved, chatter is almost unavoidable unless special suppression techniques are used or the material-removal rate is substantially reduced.

There are also four different mechanisms of machining chatter: variable friction; regeneration; mode coupling; and thermomechanics of chip formation. These mechanisms, however, are interdependent and can generate different types of chatter simultaneously; however, there is not a unified model capable of explaining all phenomena observed in machining practice.

Metal-cutting processes involve a number of strongly nonlinear phenomena which can be classified into two distinct dynamical systems, namely mechanics and thermodynamics of chip formation. Functional interrelationships between these two systems

are shown in figure 8 in the form of a closed-loop model. The proposed system can accommodate all sorts of nonlinearities; in particular, strain hardening and softening (Hastings *et al.* 1980), thermal softening (Davies *et al.* 1997), strain-rate dependence (Oxley 1963; Oxley & Hastings 1976, 1977), variable friction (Wiercigroch 1997), heat generation and conduction, feed drive hysteresis, intermittent tool engagement (Tlusty & Ismail 1981), structural and contact stiffness in MTS (Hanna & Tobias 1969), and time delay (Stépán 1998).

To illustrate the problem of chatter in real engineering practice, a case study on chatter suppression in milling using an analytical model for milling stability has been presented. The time-varying dynamics of the system is approximated using only the constant term in the Fourier series expansion of the periodically varying directional coefficients. The resultant analytical expression is demonstrated to predict the stability limit accurately. This is mainly due to the relatively slow growth of regenerative chatter, which seems to be insensitive to the higher harmonics. Application of the model to the stability of variable pitch cutters results in an analytical expression for the optimal pitch angles. The model eliminates the need for time-consuming numerical simulations in optimizing cutting conditions and tool geometry in order to maximize the chatter-free material-removal rate.

References

Abakumov, A. M, Vidmanov, Yu. I. & Mikhelkevich, V. N. 1972 An algorithm for calculating the dynamic characteristics of longitudinal turning. *Stanki i Instrument* **9**, 29–31. (In Russian.)

Altintas, Y. & Budak, E. 1995 Analytical prediction of stability lobes in milling. *Ann. CIRP* **44**, 357–362.

Altintas, Y., Engin, S. & Budak, E. 1999*a* Analytical stability prediction and design of variable pitch cutters. *Trans. ASME J. Manufact. Sci. Engng* **121**, 173–178.

Altintas, Y., Shamoto, E., Lee, P. & Budak, E. 1999*b* Analytical prediction of stability lobes in ball end milling. *Trans. ASME J. Manufact. Sci. Engng* **121**, 586–592.

Armarego, E. J. A. & Whitfield, R. C. 1985 Computer based modelling of popular machining operations for force and power predictions. *CIRP Ann.* **34**, 65–69.

Arnold, R. N. 1946 Mechanism of tool vibration in cutting steel. *Proc. Inst. Mech. Engrs (Lond.)* **154**, 261–276.

Bailey, J. A. 1975 Friction in metal machining—mechanical aspects. *Wear* **31**, 243–275.

Boothroyd, G. 1975 *Fundamentals of metal machining and machine tools*. McGraw-Hill.

Budak, E. 1994 The mechanics and dynamics of milling thin-walled structures. PhD thesis, University of British Columbia.

Budak, E. & Altintas, Y. 1998 Analytical prediction of chatter stability in milling. Part I. General formulation. Part II. Application to common milling systems. *Trans. ASME J. Dynamic Systems Measurement Control* **120**, 22–36.

Budak, E. & Kops, L. D. 2000 Improving productivity and part quality in milling of titanium based impellers by chatter suppression and force control. *CIRP Ann.* **49**, 31–36.

Budak, E., Altintas, E. & Armarego, E. J. A. 1996 Prediction of milling force coefficients from orthogonal cutting data. *Trans. ASME J. Manufact. Sci. Engng* **118**, 216–224.

Cook, N. H. 1959 Self-excited vibrations in metal cutting. *Trans. ASME J. Engng Industry* **81**, 183–186.

Cook, N. H. 1966 *Manufacturing analysis*. Redwood City, CA: Addison-Wesley.

Creveling, J. H., Jordan, T. F. & Thomsen, E. G. 1957 Some studies of angle relationships in metal cutting. *Trans. ASME* **79**, 127–138.

Cumming J. D., Kobayashi S. & Thomsen E. G. 1965 A new analysis of the forces in orthogonal metal cutting. *Trans. ASME J. Engng Industry* **87**, 480–486.

Davies, M. A., Burns, T. J. & Evans, C. J. 1997 On the dynamics of chip formation in machining hard matterrials. *Ann. CIRP* **46**, 25–30.

Doi, S. & Kato, S. 1956 Chatter vibration of lathe tools. *Trans. ASME* **78**, 1127–1134.

Eggleston D. M., Herzog R. & Thomsen E. G. 1959 Observations on the angle relationships in metal cutting. *Trans. ASME J. Engng Industry* **81**, 263–279.

Grabec, I. 1988 Chaotic dynamics of the cutting process. *Int. J. Mach. Tools Manufact.* **28**, 19–32.

Hahn, R. S. 1953 Metal-cutting chatter and its elimination. *Trans. ASME* **75**, 1073–1080.

Hamdan, M. N. & Bayoumi, A. E. 1989 An approach to study the effects of tool geometry on the primary chatter vibration in orthogonal cutting. *J. Sound Vib.* **128**, 451–469.

Hanna, N. H. & Tobias, S. A. 1969 The non-linear dynamic behaviour of a machine tool structure. *Int. J. Mach. Tools Des. Res.* **9**, 293–307.

Hanna, N. H. & Tobias, S. A. 1974 A theory of nonlinear regenerative chatter. *Trans. ASME J. Engng Industry* **96**, 247–255.

Hastings, W. F., Mathew, P. & Oxley, P. L. B. 1980 A machining theory for predicting chip geometry, cutting forces, etc., from material properties and cutting conditions. *Proc. R. Soc. Lond.* A **371**, 569–587.

Jemielniak, K. & Widota, A. 1988 Numerical simulation of non-linear chatter vibration in turning. *Int. J. Mach. Tools Manufact.* **29**, 239–247.

Kalmar-Nagy, T., Stépán, G. & Moon, F. C. 2001 Subcritical Hopf bifurcations in the delay equation model for machine tool vibrations *Nonlinear Dynamics.* (In the press.)

Kaneko, T., Sato, H., Tani, Y. & O-hori, M. 1984 Self-excited chatter and its marks in turning. *Trans. ASME J. Engng Industry* **106**, 222–228.

Kegg, R. L. 1965 Cutting dynamics in machine tool chatter. *Trans. ASME J. Engng Industry* **87**, 464–470.

Kegg, R. L. 1969 Chatter behavior at low cutting speed. *Ann. CIRP* **17**, 97–106.

Knight, W. A. 1970 Some observation on the vibratory metal cutting process employing high speed photography. *Int. J. Mach. Tools Des. Res.* **10**, 221–247.

Koenigsberger, F. & Tlusty, J. 1967 *Machine tool structures, I. Stability against chatter.* Oxford: Pergamon.

Komvopoulos, K. & Erpenbeck, S. A. 1991 Finite element modelling of orthogonal metal cutting. *Trans. ASME J. Engng Industry* **113**, 253–267.

Kudinov, V. A. 1955 Theory of vibration generated from metal cutting. In *New technology of mechanical engineering*, pp. 1–7. Moscow: USSR Academy of Sciences Publishing House. (In Russian.)

Kudinov, V. A. 1963 Dynamic characteristics of the metal cutting process. *Stanki i Instrument* **10**, 1–7. (In Russian.)

Kudinov, V. A. 1967 *Dynamics of machine tools.* Moscow: Mashinostrojenie. (In Russian.)

Lee, E. H. & Shaeffer, B. W. 1951 Theory of plasticity applied to problems of machining. *Trans. ASME J. Appl. Mech.* **18**, 405–413.

Lin, J. S. & Weng, C. I. 1991 Nonlinear dynamics of the cutting process. *Int. J. Mech. Sci.* **33**, 645–657.

Loladze, T. H. 1952 *Chip formation during metal cutting.* Moscow: Maszgiz. (In Russian.)

Magnus, W. & Winkler, S. 1966 *Hill's equation.* Wiley.

Marui, E., Kato, S., Hashimoto, M. & Yamada, T. 1988*a* The mechanism of chatter in a spindle–workpiece system. Part 1. Properties of self-excited vibration in spindle–workpiece system. *Trans. ASME J. Engng Industry* **110**, 236–241.

Marui, E., Kato, S., Hashimoto, M. & Yamada, T. 1988*b* The mechanism of chatter in a spindle–workpiece system. Part 2. Characteristics of dynamic force and vibrational energy. *Trans. ASME J. Engng Industry* **110**, 242–247.

Marui, E., Kato, S., Hashimoto, M. & Yamada, T. 1988*c* The mechanism of chatter in a spindle–workpiece system. Part 3. Analytical considerations. *Trans. ASME J. Engng Industry* **110**, 248–253.

Merchant, M. E. 1944 Basic mechanics in the metal cutting process. *Trans. ASME J. Appl. Mech.* A **11**, 168–175.

Merchant, M. E. 1945*a* Mechanics of metal cutting process. Part I. Orthogonal cutting and a type-2 chip. *J. Appl. Phys.* **16**, 267–275.

Merchant, M. E. 1945*b* Mechanics of metal cutting process. Part II. Plasticity conditions in orthogonal cutting. *Trans. ASME J. Appl. Mech.* A **11**, 318–324.

Merritt, H. E. 1965 Theory of self-excited machine-tool chatter. *Trans. ASME J. Engng Industry* **87**, 447–454.

Minis, I. & Yanushevsky, T. 1993 A new theoretical approach for the prediction of machine tool chatter in milling. *Trans. ASME J. Engng Industry* **115**, 1–8.

Minis, I., Yanushevsky, T., Tembo, R. & Hocken, R. 1990 Analysis of linear and nonlinear chatter in milling. *Ann. CIRP* **39**, 459–462.

Moriwaki, T. & Narutaki, R. 1969 Chatter stability at low cutting speeds. *J. Japan Soc. Precision Engng* **17**, 97–106.

Nayfeh, A. H., Chin, C.-M. & Pratt, J. 1997 Perturbation methods in nonlinear dynamics—applications to machining dynamics. *Trans. ASME J. Manufact. Sci. Engng* **119**, 485–493.

Opitz, H. 1968 Chatter behavior of heavy machine tools. Quarterly Technical Report No. 2 AF61 (052)-916. Research and Technology Division, Wright-Patterson Air Force Base, OH.

Opitz, H. & Bernardi, F. 1970 Investigation and calculation of the chatter behavior lathes and milling machines. *Ann. CIRP* **18**, 335–343.

Oxley, P. L. B. 1963 Shear angle solution based on experimental shear zone and tool-chip interface stress distribution. *Int. J. Mech. Sci.* **5**, 41–47.

Oxley, P. L. B. & Hastings, W. F. 1976 Minimum work as a possible criterion for determining the frictional conditions at the tool/chip interface in machining. *Phil. Trans. R. Soc. Lond.* A **282**, 565–584.

Oxley, P. L. B. & Hastings, W. F. 1977 Predicting the strain rate in the zone of intense shear in which the chip is formed in machining from the dynamic flow stress properties of the work material and the cutting conditions. *Proc. R. Soc. Lond.* A **356**, 395–410.

Piispanen, V. 1937 Theory of chip formation. *Teknillinen Aikaauslenti* **27**, 315–322. (In Finnish.)

Piispanen, V. 1948 Theory of formation of metal chips. *J. Appl. Phys.* **19**, 876–881.

Recht, R. F. 1985 A dynamic analysis of high-speed machining. *Trans. ASME J. Engng Industry* **107**, 309–315.

Slavicek, J. 1965 The effect of irregular tooth pitch on stability of milling. In *Proc. 6th MTDR Conf., Manchester, September*, pp. 15–22. Oxford: Pergamon.

Smith, S. & Tlusty, J. 1993 Efficient simulation programs for chatter in milling. *Ann. CIRP* **42**, 463–466.

Sridhar, R., Hohn, R. E. & Long, G. W. 1968*a* General formulation of the milling process equation. *ASME J. Engng Industry*, 317–324.

Sridhar, R., Hohn, R. E. & Long, G. W. 1968*b* Stability algorithm for the general milling process. *Trans. ASME J. Engng Industry*, 330–334.

Stépán, G. 1998 Delay-differential equation models for machine tool chatter. In *Dynamics and chaos in manufacturing processes* (ed. F. C. Moon), pp. 165–191. Wiley.

Taylor, F. W. 1907 On the art of cutting metals. *Trans. ASME* **28**, 31–248.

Tlusty, J. 1986 Dynamics of high speed milling. *Trans. AMSE J. Engng Industry* **108**, 59–67.

Tlusty, J. & Ismail, F. 1981 Basic non-linearity in machining chatter. *Ann. CIRP* **30**, 21–25.

Tlusty, J. & Polacek, M. 1963 The stability of machine tools against self excited vibrations in machining. In *International research in production engineering*, pp. 465–474. ASME.

Tlusty, J., Ismail, F. & Zaton, W. 1983 Use of special milling cutters against chatter. NAMRC 11, University of Wisconsin, SME, pp. 408–415.

Tobias, S. A. 1965 *Machine tool vibrations*. Wiley.

Tobias, S. A. & Fishwick, W. 1958 The chatter of lathe tools under orthogonal cutting conditons. *Trans. ASME* **80** 1079–1088.

Vanherck, P. 1967 Increasing milling machine productivity by use of cutters with non-constant cutting edge pitch. In *Proc. 8th MTDR Conf., Manchester*, pp. 947–960.

Weck, M., Altinas, Y. & Beer, C. 1994 CAD assisted chatter-free NC tool path generation in milling. *Int. J. Mach. Tools Manufact.* **34**, 879–891.

Wiercigroch, M. 1994 A numerical method for calculating dynamic responses in the machine tool-cutting process system. *Archive Mech. Engng* **41**, 29–38.

Wiercigroch, M. 1995 Complex dynamics of a simple machine tool-cutting process system. *Archive Mech. Engng* **42**, 151–165.

Wiercigroch, M. 1997 Chaotic vibrations of a simple model of the machine tool-cutting process system. *Trans. ASME J. Vib. Acoustics* **119**, 468–475.

Wiercigroch, M. & Cheng, A. D.-H. 1997 Chaotic and stochastic dynamics of metal cutting process. *Chaos Solitons Fractals* **8**, 715–726.

Wright, P. K. 1982 Predicting the shear plane angle in machining from workmaterial strain-hardening characteristics. *Trans. ASME J. Engng Industry* **104**, 285–292.

Wu, D. W. 1986 Governing equations of the shear angle oscillation in dynamic orthogonal cutting. *Trans. ASME J. Engng Industry* **108**, 281–287.

Wu, D. W. 1988 Comprehensive dynamic cutting force model and its application to wave-removing processes. *Trans. ASME J. Engng Industry* **110**, 153–161.

Wu, D. W. & Liu, C. R. 1985a An analytical model of cutting dynamics. Part 1. Model building. *Trans. ASME J. Engng Industry* **107**, 107–111.

Wu, D. W. & Liu, C. R. 1985b An analytical model of cutting dynamics. Part 2. Verification. *Trans. ASME J. Engng Industry* **107**, 112–118.

Zharkov, I. F. 1985 *Vibration in metal cutting*. Moscow: Mashinostrojenie. (In Russian.)

Zorev, N. N. 1956 *Questions asked from mechanics of the metal cutting processes*. Moscow: Mashinostrojenie. (In Russian.)